38503

Report of Committee III in Preparation for the Clear Channel Hearing, Docket #6741

PART I

January 15,1946

This Committee was appointed at the Informal Engineering Conference of March 16, 1945 to consider the "Determination of distances to which and areas over which various signal strengths are delivered".

The satisfactory solution of this problem demands adequate information as to the ranges of both the ground wave and the skywave under all operation conditions, over all varieties of terrain and throughout all the phases of cyclical variations to which they are subject.

With regard to the ground wave it seems to be the general concensus and is the opinion of the Committee that the determination of its ranges as at present set forth in the Commission's Standards of Good Engineering Practice are adequate and stand in no need of revision except in respect to the ground conductivity map. The revision of this map was therefore placed on the agenda of the Committee and the profession circularized to obtain pertinent information. However, owing to the shortage of qualified personnel, the heavy work load on the Commission's engineering staff and the magnitude of the task of analyzing the sky wave data, practically nothing has been done toward the preparation of a ground conductivity map. The Committee is of the opinion that the preparation of this map is one of the essentials to the satisfactory solution of the problem as a whole and recommends that it be undertaken as soon as possible. It is estimated that the work required would amount to six man-months of engineering--not clerical-time.

With regard to the sky wave, the situation is quite different from that of the ground wave. The field strength vs distance curves of the Standards of Good Engineering Practice were based on the results of a three months'recording program carried out as a cooperative enterprise by the Commission and the industry in the late winter and early spring of 1935. This was a period just beyond a time of a sunspot minimum. Since then we have passed through a sunspot maximum and another minimum, for a considerable portion of which time the Commission has maintained a recording program at a number of its monitoring stations on a selected number of transmitting stations. While, until the formation of this Committee these recordings had not been systematically analyzed, cursory inspection of a few served to confirm the general expectation that considerable departures from the results of the 1935 survey could be expected especially at the period of a sunspot maximum.

Thus the analysis of the accumulated hundreds of thousands of hours of recordings in the Commission's files was made the number one item on the Committee's agenda. The work accomplished (summarized below) has been made possible through the cordial and effective cooperation of the industry in supplementing the Commission's staff with as large a number of clerical and statustical personnel as could

be conveniently supervised. The Committee has held six meetings largely devoted to discussion of this analysis as it has progressed and in particular to those aspects which cover ground not developed in the 1935 survey, such as the night to night deviations from the median values and the effects of geographic latitude and frequency which have been found. The details of the analytical procedures and the results thus far obtained are set forth in Part II of this report.

In summarizing these results it may be stated that both the annual median field strengths and the night to night deviations from the median (which we venture to style the "stability" of the field) are functions of the latitude, the frequency on which the transmission takes place and the phase of the solar sunspot cycle at a given time.

The dependence of the annual median field for transmissions on frequencies around the middle of the standard broadcast band and for a period of sunspot minimum (1944) are depicted in Figures 5.4a, b and c of Part II. These show that the fields are greater for the lower latitudes than for the higher.

The dependence of the stabilities for the same frequency range and phase of the solar cycle are shown in Figure 5.1 of Part II. These show that the stabilities are greater (i.e., the night to night variations are less) at the lower latitudes than at the higher.

For frequencies of transmission in the standard broadcast band other than those for which the above figures can be considered as valid, the corrections required are relatively small. For the higher frequencies, both the annual median fields and the stabilities are somewhat higher than for the lower frequencies. In other words, the transmission characteristics of a station using a frequency near the upper end of the band and located in a northern latitude are the same as if it operated on a lower frequency in a more southern latitude. While such equivalences can be worked out from the data contained in this report, no convenient way of doing so has yet been worked out. It is however by no means a hopeless problem to find a simple formula for accomplishing it.

As to the effect of the phase of the solar cycle on the propagation at given latitudes, it may be stated that the effect on both the annual median values and the stabilities is relatively small at the lower latitudes and increases with the latitude. It has not been found possible to get the figures illustrating this dependence drawn in time for inclusion in this report, although the data on which they are based is presented. It is expected that these figures will be ready by February 15.

From this brief description of the major results of this analysis of upwards of a quarter of a million of hours of recordings, it will be seen that the problem of deducing from them simple working rules for practical use in allocation engineering is a very difficult one even if no other considerations than those of the propagation characteristics are taken into account. But we know that the

advantages from the propagation standpoint of the lower latitudes shown by the survey will be seriously lessened by the higher noise levels prevalent at those latitudes. So the best answer to the whole problem would appear to depend on a careful correlation of the results of the work of Committee I with those of this Committee.

Thus Committee III feels that although it may be possible to base standards on its present results which would be some improvement on the Commission's present standards, it would be the port of wisdom to continue and adequately correlate the work of both Committees.

While the data at hand in the Commission's files has proved in general to be adequate, in one respect the Committee feels that it should be supplemented. For a satisfactory determination of the boundaries of areas of violent fading, and of interference between closely spaced stations, more field strength measurements at distances of from 50 to 250 miles from the transmitter are necessary. Hence, in addition to a continuing study of the data at hand, the Committee recommends the initiation of a recording project to supply this deficiency.

PART II

The data heretofore available on the fading and the range of skywave signals of medium frequency is largely that contained in the report of the 1935 Broadcast Allocation Survey, the conclusions of which are summarized for allocation purposes in Figure 1, Appendix 1 of the FCC Standards of Good Engineering Practice. This figure shows the values that the skywave field intensity is expected to exceed for various distances during the second hour after sunset at the recording station. The fundamental data resulted from measurements over some 500 transmission paths at frequencies from 640 Kc. to 1190 Kc. in the interval from February to May.

During 1938 the Engineering Department of the Federal Communications Commission began the Sunspot Cycle Recording Project, a program of intensive recording of skywave at medium frequencies, over a few selected paths. The object of this program has been, in particular, to discover the nature and extent of the effect of sunspot activity on skywave propagation as this activity varies through maxima and minima and, in general, to discover any possible improvements in the skywave propagation curves used for predicting service and interference in medium frequency broadcast allocation.

1. Origin of the Data.

Receiving stations are located in the vicinities of Baltimore Maryland, Atlanta, Ga., Grand Island, Neb., and Portland, Oregon.

At each station, fields are received on a vertical wire antenna by one or more superheterodyne receivers. The automatic volume control characteristics of the receivers make their output approximately a logarithmic function of the input signal and provide a useful working range of approximately 1000 to 1.

Each antenna was calibrated by determining the receiver response, at the recording chart, to signals from a standard signal generator and, subsequently, by recording ground waves at a number of frequencies from nearby stations at the same time measuring the field intensities of the ground waves with a standard field intensity meter. The result of these measurements for each antenna is an Antenna Calibration Curve showing antenna effective height as a function of frequency. The effective heights in use are of the order of 10 meters.

At first, recordings were made as directly as possible of the detected carrier. This gave a record, it is believed, of something close to the instantaneous values of the skywave; however, because of the rapid fading it also gave a record especially tedious to analyze. As it had already been determined that the variation of the instantaneous field within the hour is determined accurately enough by the Rayleigh distribution (see the appended "Notes on Probability Functions") so that it is necessary to analyze an hour's recording for only one statistic, an investigation was made to see if the insertion of a smoothing circuit between the receiver

and recorder would affect the indicated hourly median values. Simultaneous recordings with and without long time constant determined that a resistance-capacity circuit of time constant of about 60 to 100 seconds could be safely inserted between the receiver and recorder without disturbing the hourly median values. Accordingly, toward the end of 1939 these circuits were put in use on all recorders.

The Receivers are housed in small booths beside the antennas and are located in clearings free of obstructions and wiring. The receivers are supplied with power from voltage regulators. The considerable heat generated by the equipment in the small booth together with the adjustable ventilation louvres and rather large thermal capacity of the equipment aid in minimizing temperature variations.

Calibration of the receivers is checked from time to time and new calibration curves are drawn whenever a calibration is found to differ from the last one at any level by more than 5%.

On a few of the transmission paths recordings were made daily, most recordings, however, were made on a periodic basis switching the receiver through a cycle of three or four stations, recording each station five days continuously out of fifteen or one day out of four.

The charts were analyzed hour by hour for median field intensity on a suntime basis. Through 1941 the sunset hour was taken to be the hour centered on the later of the sunsets at the two ends of the transmission path. From 1941 through 1945 the sunset hour has been that centered on sunset time at the midpoint of the path.

2. The Data and Nomenclature.

It is the purpose of this section to summarize the annual data thus far available from the Recording Project, unaffected as far as may be by assumption or conclusion, and to introduce some nomenclature that has proved convenient.

Of the notoriously many ranges of statistical variability of the skywave, from moment to moment, from hour to hour, and so on, only three are studied here in detail:

1. Variation of the instantaneous field in intervals of an hour;
2. Variations of the hourly median field intensity from night-to-night in intervals of a year;
3. Variation of annual statistics from year to year.

In order to distinguish numbers from these various ranges conveniently the following symbolism is used:

E is used to denote a value of the instantaneous field intensity;

$E_{p\%}$ is used to denote a value exceeded by the instantaneous field for p% of the hour, but

E_m is used for the median value (i.e. $E_{50\%}$);

$E_{mp\%}$ is used to denote a value exceeded by the E_m fields on p% of the nights of the year, but

E_{mm} is used for a median value of a set of E_m fields;

E_{ma} is used for an average of a set of E_m fields.

The older time reference has been adopted for this report and the notation SS+2 will be used to refer to the second hour after sunset, where the sunset hour is the hour centered on the later of the sunset times at the two ends of the path.

Figure 2.1 lists the E_{ma} SS+2 values for each path and for each year for which there was recording available for three quarters of a year or more. Those averages depending on less than a year's recording are marked (P). The unattenuated field in millivolts per meter at one mile from an antenna 0.311λ in height and radiating the same amount as the antenna in question at the angle pertinent to transmission by one reflection, usually called the equivalent 0.311λ radiation, is shown at the extreme right. If the radiation was changed in the course of the recording, the radiation value appropriate to an average value is indicated by means of superscript letters. In 1942, '43 and '44 when the time reference was at the path-midpoint, values in SS+2 on the adopted time reference have been obtained from diurnal curves for the individual paths. On the longer paths where the signals sometimes fell to low enough values to be masked by the local noise, an estimate has been made of the upper and lower bound to the average: the upper bound is taken to be the average of the clear signals, the lower bound is then obtained by assuming that the instances of signal obscured by noise were instances of zero signal and forming the resultant average. These two values are shown in brackets on the longer paths.

Figure 2.2 shows the extent of the night-to-night fading of the SS+2 E_m fields in terms of the ratio of the E_{mp} values to the E_{ma} values; that is, the table shows the multiple of the annual average value to which (or beyond which) the E_m fields rose on various numbers of nights (shown in percent of the year)

These distributions are composite and were constructed as follows: A scheme of 32 classes was used in which to tally the frequency of occurrence of fields at various levels. The classes were defined by levels which are multiples of the E_{ma}

value for the year whose fields were classified. This scheme of classification provided, at the same time, a distribution by absolute field intensity and by ratio to the annual average value. The distributions by absolute value of course, varied from year to year. The variation from year to year of the distribution by ratio was expected to be much less and proved to be small enough to be wholly indeterminate by the quantity of data available. (cf. Sec.5 below) Accordingly, the frequency of occurrence of fields in the various classes were combined from year to year to determine the composite ratio distributions shown.

It seems impractical to report all the many available diurnal curves; however, Figures 2.3 and 2.4 show two composite diurnal curves: one for Long East-West paths and one for North-South and short East-West paths. The ratio of the E_{ma} field received in each evening hour to the value received in the second hour after sunset was computed for each of 9 paths for 1943 and for 1944. The 1943 set of values is plotted as dots to the left of the hour line and the 1944 set of values to the right. The median value of each set of dots is plotted on the hour line by a cross. Figure 2.5 identifies the paths and data considered.

3. Some Graphical Displays of the Data.

Although Section 2 gives all the fundamental data to be accounted for, it is instructive in the general interpretation of the data to consider additional graphical displays before proceeding to draw conclusions.

Figure 3.1 shows running averages of day-to-day E_m fields. The curve at the top of the figure shows a 13 day running average of G-WLW SS+3 E_m fields. This graph indicates rather definitely that in addition to the variation of received fields on account of random causes there is an underlying tendency to follow a cyclic variation with a period of approximately 27 days. There is also an indication, considering the fairly strong smoothing effect of a 13 day span, that in the course of approximately 27 days the field received over a given path may vary through about as great a range as it does throughout the year.

From this figure the qualitative and precautionary conclusion is drawn that "27 day" cyclic variations probably exist in medium frequency skywave fields and that in consequence short-term averages (of the order of a month, more or less) are likely to be affected by systematic involvements introduced by the span of the average as well as by the large probable error incidential to statistics of small samples of wide spread.

The lower curves of Figure 3.1 show 90-day running averages of B-WLW SS+3 E_m fields. One graph shows the running average for a 90-day period of daily data, the other shows the running average for a 90-day period using data from every fourth day of recording. These graphs show a comparison between one possible set of averages that would have been obtained had this path been recorded on the one day out of four basis and what was actually obtained from daily records. The disagreement runs, in this case, through a range ±25%. Since there is no reason to believe that this disagreement is unusual, it appears that it is inadvisable to derive statistics from seasonal samples of data from every fourth day.

It is notable in Figure 3.1 that in mid-winter the curves go to a minor minimum rather than to a maximum. A few other graphs such as these have been made for other paths and the appearance of the winter minimum appears to be typical although it is variable in depth.

Figure 3.2 shows graphically the nature of an annual sample of SS+2 E_m fields fairly typical of central U. S. latitude. The fields are those received over the G-KOA path. The number of days on which recordings were made is shown at the top of each sample. In the first three years recordings were made one day out of four and in the last three years, five days out of fifteen.

As far as one is justified in concluding from this figure, the spread of the annual sample is the same from year to year regardless of the phase of the sunspot cycle. One year in the sunspot cycle will be distinguished from another chiefly in the central statistics such as the average value, the median value, the most probable value, etc., these values rising in "good" years and falling in "poor" ones.

Figure 3.3 is similar to Figure 3.2, showing however, monthly SS+2 samples recorded over the G-KOA path. This figure together with 3.1 illustrates the extent of seasonal trend. Seasonal trend is clearly detectable but is of minor significance when compared with the random variation or with the "27 day" cyclic variation.

Figure 3.4 illustrates the extent to which the portion of the E-layer between Cincinnati and Atlanta is simultaneously good or poor for propagation with the portion between Cincinnati and Baltimore. Each dot in the figure represents that on some day E_m fields of the indicated values were received simultaneously in SS+2 over the B-WLW and A-WLW paths.

That there is some correlation between the two signals is evident. The more important observation, however, is that the signals on these two paths whose mid-points are separated only 300 miles, is as low as it is. It appears plausible to

assume, for practical purposes, that there would be no correlation between signals arriving over paths as remote from each other as are those followed by a desired service signal and by an undesired interfering signal.

Figure 3.5 shows the SS+2 E_{ma} values for 1944 spotted against a graph of the Allocation Survey 50% Curve (Figure 1, Appendix 1 of the FCC Standards of Good Engineering Practice).

4. Sample Size, Precision of Statistics.

Examination of Figure 3.2, showing the annual samples of G-KOA E_m fields, indicates immediately that on account of the large range involved, even the largest possible sample with 365 data would still be a small one for purely statistical purposes. On the other hand, examination of Figure 2.2 or Figure 5.1, showing the range of the annual samples on various transmission paths, suggests that a sample of a given number of data is effectively larger for some transmission paths than for others.

Examining Figure 3.2 again, it is quite plausible to assume that the exact position of any one of the dots is, within some limits, a random matter; or, put a little more precisely, if the total range of variation is divided into a number of smaller ranges the number of dots in any one range will, from sample to sample, be expected to vary at random according to the simple normal law about an "expected number" determined by the actual distribution law.

Figure 4.1 shows on the left, the ratio distribution curves obtained for the G-KOA data for 1939, 1940, 1941 and 1942. (The curves for 1943 and 1944 are similar to these although a little less variable. They have been omitted so as to leave the tangle of curves barely readable). The significance, from a statistical point of view, of the scatter of these curves may be examined as follows: The actual distribution law in each of the years was certainly something like the composite law $P_c(R)$, curve A to the right in Figure 4.1. If it be assumed that P_c was the actual distribution law in operation and if it be assured, as in the paragraph above, that fields were distributed in small ranges normally at random, it is then possible to apply Pearson's criterion for goodness of fit to determine the probability that with a law such as P_c in operation, a distribution such as that in 1941 (as unusual as it is) might occur. This probability turns out to be approximately 33%. (The sub-ranges for R used in the test were the twenty ranges defined by P_c as containing, each, 5% of the data. The resultant value of χ^2 is 20.15).

Thus, from a statistical point of view, the scatter of the ratio distribution curves in the various years cannot be affirmed to have any significance and, lacking any other information, the scatter of the curves should be assumed to have none. On the other hand, of course, the probability computation does not deny significance to the scatter of the curves,

but merely asserts that, considering the nature of the data and their number, the annual ratio distribution curves cannot be "resolved" by statistical methods. Had the 1941 curve been as shown but determined by as much as twice as many data the probability of its occurring if the law P_c were in operation would have been less than 1%; and had this occurred, there would be serious doubt that P_c was in operation in 1941 and, consequently, serious doubt would be cast upon the validity with which composite distributions can characterize even the present data.

It is more difficult to estimate the possible error in the determination of the statistics of the fields recorded along the various paths. No estimate has been made for any except the average.

The distribution of the fields about the average is very far from normal so that estimates of the error in terms of the standard deviation are doubtful. For this reason in addition to standard errors, certain other errors (see below) have been computed that are more directly related to the distribution laws at hand.

The standard deviation of the G-KOA $P_c(R)$ has been computed to be 0.749 so that the standard error for G-KOA is 7.9% or 5.9% respectively for samples consisting of 90 data or 160 data.

On the other hand, the error incidental to a plausible but extremely high sample has been computed. This "maximal" sample is defined as follows: The range of R is divided into 20 sub-ranges defined by $P_c(R)$ as containing, each, 5% of the data. It is then supposed that, for the sample in question, each of the lower ten sub-ranges has lost an equal number of data while each of the upper ten sub-ranges has gained them. The number of data so "transferred" being subject to the restriction that the resultant distribution shall not be unusual with a probability of more than 50% by Pearson's criterion of goodness of fit. That such a sample is plausible is assured by the 50% measure, yet that it is extreme is clear from the great uniformity assumed for the irregularity.

Curve B of the curves to the right in Figure 4.1 represents the actual distribution of such an maximal sample of 90 data as derived from $P_c(R)$. From it the average can be determined to be 27% high. If such a sample actually occurred its average would not necessarily be recognized to be high and, in any case, its distribution would be referred to the actual average as a unit so that the distribution curve for the year in which it occurred would appear as curve C. This curve may be compared with the year to year curves for unusualness. For maximal sample of 160 data the same process gives 20% as the error.

In Figure 5.1 of the next section of this report the data of Figure 2.2 is interpreted to mean that the night-to-night fading of E_m fields is chiefly a function of latitude. The methods used above to determine the standard error and the maximal error may be applied at various latitudes to determine the following tables:

STANDARD PERCENT ERROR

No. of data in annual sample	Latitude		
	35°	40°	45°
90	2.83	7.84	10.7
160	2.12	5.88	8.02
365	1.40	3.89	5.31

MAXIMAL PERCENT ERROR

No. of data in annual sample	Latitude		
	35°	40°	45°
90	14.3	26.2	32.1
160	10.7	19.8	24.8
365	6.7	13.2	16.6

The standard error is rather abstract with respect to the statistical realm of concern here, while the concept of the maximal sample as defined, at least, bears an easily pictured physical relationship with actual recorded samples. With this physical relationship in mind it appears reasonable to expect that errors as large as the maximal ones can be expected to occur rarely but that more typical ones would be between the standard errors and the maximal ones.

5. Derived Fading and Signal Range Curves.

The description of the night-to-night fading of the hourly median fields, the function that gives the probability that the field will exceed a value E_m is dependent on four parameters:

$$(1) \qquad P(E_m;\ \theta,\ f,\ d,\ S),$$

latitude, frequency, path length, and a factor dependent on the phase of the sunspot cycle. For the determination of such a highly contingent function the available data is very limited indeed and to determine even a practical approximation to it requires the use of rather indirect methods.

As was implied in sections 2 and 4 above the assumption has been made that the annual E_{ma} value will rise and fall from year to year, with the sunspot cycle factor S and that the other statistics will rise and fall with E_{ma} so that if the E_m fields are measured with E_{ma} as a unit, the distribution of the ratio $R = E_m/E_{ma}$ will be independent of S:

$$(2) \qquad P(R;\ \theta,\ f,\ d)$$

This assumption is surely quite accurate with respect to statistics centrally located in the range of variation of E_m. There is some indication, however, that some of the more extreme statistics may not satisfy the assumption. For example, there is some indication that $E_{m10\%}$ may vary very little from year to year.

Figure 2.3 shows the empirically determined ratio distribution functions of the sort (2) above for various combinations of the parameters θ, f and d. Of these parameters it is clear that θ is the one of major importance. The R values for each tabulated value of P(R) (that is, the figures from each column of Figure 2.3) have been graphed versus latitude and curves have been determined which appear to typify the data best. These curves are shown in Figure 5.1. It was possible to draw these typical curves down through the data very satisfactorily "averaging" out the effects of f and of d without giving special weight to any datum except for those from the paths P-WSB and P-WENR. Even the data from these paths required no special treatment for the 5, 10, 20 and 30% curves. For the higher percentage curves, however, the data from these paths seemed definitely to fall below the trend rather clearly established by the rest. These data then were given only very light weight in the determination of the curves of Figure 5.1.

The process of derivation of Figure 5.1 appears actually to have averaged out a frequency effect while it is somewhat doubtful whether there was any effect of path-length to be removed. Examination of the way in which the data of Figure 2.3 deviate from the curves of Figure 5.1 indicates that these curves represent best the fading behavior versus latitude of frequencies in the neighborhood of 1000 Kc. Frequencies above 1000 Kc., over a given path, fade from night to night as if the path were at a lower latitude by an amount roughly proportional to the increment of frequency over 1000 K and to the increment of latitude over some low latitude, .35° or less. However, the magnitude of this frequency correction in terms of latitude under the most favorable conditions (highest broadcast frequency and highest U. S. latitude) appears to be only of the order of 2.5° to 3.0° and usually amounts to a degree or less.

A frequency effect of this sort seems certain of existence but in view of the fact that an effect of this magnitude is not of practical urgency, although it is of practical importance, it seems desirable to leave any numerical formulation of it until further study can be made.

Having discovered a decided latitude effect in the probability functions that describe the distribution of fields, an effect is to be expected in the annual average values. Figure 3.5 showing a plot of the 1944 E_{ma} values together with the Allocation Survey Curve shows such an effect, data from low latitude paths falling regularly above the curve and those from high latitude paths below. At the same time, it is to be noted that the Survey Curve does appear typical of the data and, considering its extensive basis, may very plausibly be expected to represent some "average"latitude. This is particularly fortunate for it is obvious that it would be most difficult and uncertain to derive such a curve from the present data.

Assuming the Survey Curve to give the proper shape of the E_{ma} versus distance graph and that it is at the proper level for some latitude (in 1944), it is possible to study the deviations of the 1944 data from this curve to determine the latitude of which it is most characteristic and to derive curves for other latitudes.

To determine similar curves for other years requires the study of year-to-year variation of annual statistics. In this realm of variation data are, of course, yet scarcer. Study of these variations have not yet been brought to a conclusion, but it is hoped at an early date to add to this report an annex in which such conclusions will be drawn as are possible at this time.

In order to obtain the correlation with latitude of the deviations of the 1944 data from the Survey Curve, it is necessary to discount the exaggeration of effects per reflection in transmissions involving multiple reflections. It was at first assumed, in order to make a rough test, that the ratio of the actual E_{ma} field to that predicted by the curve might be taken to measure effects per reflection at short distances, and that at longer distances, where transmission by two reflections would be predominant, the square root of this ratio could be taken. The result of this test was quite favorable, so it became necessary to find a means of expressing this exponent as a function of distance so as to remove its discontinuity. It was supposed that if it were discovered that the ratio of the actual field intensity per reflection to the value predicted by the Survey Curve were D at some latitude θ then the field intensity at various distances would be expressed in terms of the Survey Curve by the expression

$$\frac{E_{\theta}(d)}{E_{Sur}(d)} = D^{\chi(d)}$$

As long as the value of D is near unity the value of α is by no means critical. A value for the function $\alpha(d)$ has been obtained from Figure 2 of an essay entitled "Supplementary Report on Wave Propagation For the CCIR" by Mr. K. A. Norton. This figure shows theoretical curves expressing the field intensity received at various distances after one, two and higher numbers of reflections. Each of these curves was multiplied by 1.25^n, where n is the pertinent number of reflections, and the resultant computed. The ratio of the resultant of these augmented field intensities to that of the original ones then gave the values of $1.25^{\alpha(d)}$. Solution of this at 100 mile points gave values for a graph of $\alpha(d)$. This graph is shown in Figure 5.2 of this report. (A re-check using 1.10^n to obtain $1.10^{\alpha(d)}$ determined substantially the same function $\alpha(d)$).

Assuming then that the actual deviations per reflection of the 1944 data from the Survey Curve have been exaggerated at various distances by the exponent $\alpha(d)$, corresponding roots have been taken of the actual ratios to obtain the deviations per reflection shown in Figure 5.3. From the curve determined by these data it appears that the Survey Curve best represents E_{ma} versus distance for a latitude of about 42.3°.

From Figure 5.3 it has been determined that field intensities per reflection deviate from the Survey Curve by ratios of 1.25, 1.10, and 0.88 at latitudes of 35°, 40° and 45°, respectively. Raising these ratios to the power α gives multipliers to transform the Survey Curve into $E_{ma}(d)$ curves characteristic of the respective latitudes. Applying the ratio distributions of Figure 5.1 to these curves then gives the fading and range curves of Figure 5.4a, b, c. (Although these curves are drawn in solidly to 100 mi, they are considered to be of doubtful significance inside a distance of 250 mi.)

6. Fading and Interference Limitations to Service.

With respect to limitations to service on account of fading or on account of interference, it is believed that there is now sufficient information to permit a more practical representation of these limitations than merely in terms of a per cent of the time: viz., it is possible to describe the state of the service within the hour under fixed conditions for desired and undesired signals and, subsequently, to determine how frequently these fixed conditions will occur from night to night.

To these ends, Figure 6.1 shows the Rayleigh distribution of fading within the hour about the hourly median field, while Figure 5.1 shows the night-to-night fading of hourly median fields about their annual average. Figure 6.2 shows the per cent of the hour free of interference when the ratio

of the desired E_m is R times the undesired E_m if interference is defined to exist instantaneously when the instantaneous desired E is less than R_o (a standard, presently taken at 20) times the instantaneous undesired E. (cf. the appended "Notes on Probability Distributions", Section 3 for the derivation of the figure). Figure 6.3 shows the number of nights per year on which various ratios of desired E_m to undesired E_m fields are realized at a point where the value exceeded by the undesired field on 10% of the nights equals 1/20 the value exceeded by the desired on 50% of the nights. (cf. the appended "Notes on Probability Distributions", Section 4 for the method of derivation).

From these figures it will be seen, for example, that if 90% of the hour is to be free of interference (Figure 6.2) the ratio of the median value of the desired to the median value of the undesired should be 60 to 1; then, from Figure 10 it will be seen that at the fringe of the 500 uv/m median service area (limited by interference) a ratio of 60 to 1 or better will be realized (with the desired signal also above 500 uv/m) on approximately 10%, 31% and 39% of the nights at 35°, 40° and 45° latitude respectively. If the limitation is to a sufficiently high contour so that the service lost to fading of the desired signal itself may be ignored, the results will be seen to be a little better.

The inequity that appears here from latitude to latitude comes about because the night-to-night signals at higher latitudes fade much further below their 10% values than do signals at lower latitudes. Thus, as may be seen from the left-hand portion of Figure 6.3, the present definition of interference leads to a ratio of desired E_{mm} to undesired E_{mm} of about 30, 46 and 70 at 35°, 40° and 45° latitude, respectively.

If this ratio is made uniformly, say, 50 at every latitude the inequity at the edge of the service area disappears although it persists inside the service area. This condition may be examined in Figure 10 by sliding the R scale with respect to the % scale placing R= 50 opposite %= 50. It is interesting to note that the present Standards all together accomplish roughly this effect by under estimating both the desired and the undesired signals at low latitudes and by over estimating both at higher latitudes, as long as the desired and undesired transmission paths have approximately the same latitude.

Finally, Figure 6.4 shows theoretical curves for the distribution of the fading of the instantaneous value of the resultant of a groundwave and a skywave. These curves are derived on the assumptions that the skywave is random in phase with respect to the groundwave and is distributed in amplitude according to the Rayleigh distributions. (cf. Sec.5 of the appended "Notes on Probability Functions..." for the derivation)

SOME NOTES ON PROBABILITY FUNCTIONS AND DISTRIBUTIONS DESCRIBING FADING SERVICE AND INTERFERENCE AT MEDIUM FREQUENCIES

Notation and definitions.

In the following, script letters will be used to denote vectors and ordinary print to represent scalars.

W(E) will be used to denote the probability that a field intensity lies between E and E dE in magnitude, while W($\mathcal{E}$) will be used to denote the probability that the field intensity lies in a differential element of phase space.

P(E) will denote the probability that the field intensity is greater than E. Where it is desirable to represent the probability that the field intensity is less than E, no special function will be named. The probability will be represented simply by 1 - P(E).

To simplify the nomenclature, the two probability functions will be distinguished by calling the W functions the probabilities, and the P functions the distributions.

These functions, of course, are related by

$$P(E) = \int_E^\infty W(E)\,dE = \int_0^{2\pi} d\theta \int_E^\infty W(E)\,E\,dE$$

1. The Short Time Fading of Skywaves.

The distribution of instantaneous values of downcoming skywaves has been shown, by analysis of recordings to be

1.1 $$P(E) = e^{-\frac{E^2}{E_0^2}}$$

for a short period of time. In this expression E_0 is a constant determined by the general level about which the instantaneous field intensity E is randomly varying. The length of time for which the distribution may be considered valid is the length of time for which the wave may be considered as havinga constant"general level". To define constant general level at this point would lead to unprofitable complication; however, it may be noted that the time intervals actually studied were the fourth hours after sunset.

Immediate consequences of 1.1 are that the probability function is

1.2 $$W(E) = \frac{2E}{E_0^2}\, e^{-\frac{E^2}{E_0^2}} ;$$

so that

$$\overline{E^2} = \int_0^\infty E^2 W(E)\, dE = E_o^2 ,$$

or

1.3 $$RMS(E) = E_o ;$$

1.4 $$\overline{E} = \int_0^\infty E\, W(E)\, dE = \frac{\sqrt{\pi}}{2} E_o ;$$

and, directly from 1.1

1.5 $$\text{median}(E) = E_m = E_o \sqrt{\ell n\, 2} .$$

Thus E_o, E, or E_m (as well as other statistics) may equally well be taken as measures of the general level since there exists a simple proportionality between any two of them.

2. Distribution of the Instantaneous Amplitude of the Sum of Two or more Skywaves.

The received field intensity is physically one-dimensional but is known to be varying in phase. It is therefore generally assumed that the distribution 1.1 describes the resultant amplitude of ramdom flights in two dimensions, so that the probability in phase space is

2.1 $$W(\mathcal{E}) = \frac{1}{\pi E_o^2}\, e^{-\frac{E^2}{E_o^2}}$$

If the resultant $\mathcal{E}$ is the sum of N vectors $\mathcal{E}_n$ of individual probabilities $W_n(E_n)$, then by Markoff's method the probability that $\mathcal{E}$ is in the element of phase space $d\mathcal{E}_x\, d\mathcal{E}_y$ is

2.2
$$\begin{cases} W_N(\mathcal{E}) = \frac{1}{4\pi^2} \int_{space} e^{-i\rho\cdot\mathcal{E}}\, A_N(\rho)\, dx\, dy \\ \rho = (x, y) \\ A_N(\rho) = \prod_n^N \int_{space} W_n(\mathcal{E}_n)\, e^{i\rho\cdot\mathcal{E}_n}\, d\mathcal{E}_{nx}\, d\mathcal{E}_{ny} \end{cases}$$

In the case of immediate interest, the w_n are dependent only on the amplitudes of the ξ_n , so that the procedure 2.2 can be carried out most readily in polar coordinates:

2.3 $$W_n(\xi_n) = \frac{1}{\pi E_{on}^2} e^{-\frac{E^2}{E_{on}^2}}$$

2.4 $$A_N(r) = \prod_n^N \frac{1}{\pi E_{on}^2} \int_{space} e^{-\frac{E_n^2}{E_{on}^2}} e^{ir E_n \cos\theta} E_n \, dE_n \, d\theta$$

$$= \prod_n^N \frac{2}{E_{on}^2} \int_0^\infty J_0(r E_n) e^{-\frac{E_n^2}{E_{on}^2}} E_n \, dE_n$$

$$= \prod_n^N e^{-\frac{E_{on}^2}{4} r^2} = e^{-\frac{\Sigma E_{on}^2}{4} r^2}$$

2.5 $$W_N(\xi) = \frac{1}{4\pi^2} \int_{space} e^{-ir E \cos\theta} e^{-\frac{\Sigma E_{on}^2}{4} r^2} r \, dr \, d\theta$$

$$= \frac{1}{2\pi} \int_0^\infty J_0(rE) e^{-\frac{\Sigma E_{on}^2}{4} r^2} r \, dr$$

$$= \frac{1}{\pi \Sigma E_{on}^2} e^{-\frac{E^2}{\Sigma E_{on}^2}}$$

It follows from this and from 1.3, 1.4 and 1.5 that the RMS , the average and the median values of the resultant wave are the RSS (root of the sum of the squares) of the corresponding values for the component waves.

3. Distribution of interference between Two Fading Waves within the hour.

Let interference be defined to exist whenever the instantaneous amplitude of the desired wave E_d is less in ratio to the instantaneous amplitude of the undesired wave E_u than some standard ratio R_o :

3.1 $$R_o E_u = E_d$$

Let the ratio of the general level of the desired to undesired wave for the hour in question be R ,

3.2 $$R E_{ou} = E_{od}$$

The probability that the desired and undesired instantaneous field intensities be in the element of space indicated in the figure is

3.3 $$W(E_u, E_d) = W(E_u)\, W(E_d),$$

subject to the highly acceptable assumption that $W(E_u)$ is independent of $W(E_d)$

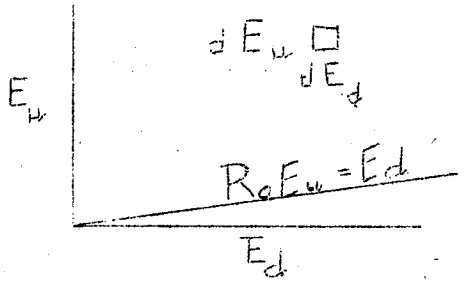

The probability of interference under the standard R_o when the general level of the desired wave is at R with respect to the undesired wave is

3.4 $$P(R, R_o) = \int_0^\infty dE_d \int_{\frac{E_d}{R_o}}^\infty W(E_u, E_d)\, dE_u$$

$$= \int_0^\infty \frac{2E_d}{E_{od}^2}\, e^{-\frac{E_d}{E_{od}^2}}\, dE_d \int_{\frac{E_d}{R_o}}^\infty \frac{2E_u}{E_{ou}^2}\, e^{-\frac{E_u^2}{E_{ou}^2}}\, dE_u$$

3.4 $$P(R, R_0) = \int_0^\infty \frac{2E_d}{E_{od}^2} e^{-\frac{E_d^2}{E_{od}^2}} e^{-\frac{E_d^2}{R_0^2 E_{ou}^2}} dE_d$$

$$= \int_0^\infty e^{-\left(1+\frac{R^2}{R_0^2}\right)\frac{E_d^2}{E_{od}^2}} \frac{2E_d}{E_{od}^2} dE_d$$

$$= \frac{1}{1+\left(\frac{R}{R_0}\right)^2}$$

In an hour when the intensity exceeded by the undesired wave for 10% of the time is exactly 1/20 of the median value of the intensity of the desired wave

$$E_{10\%u} = \frac{1}{20} E_{md} = 1.823\, E_{mu},$$

$$E_{mu} = \frac{1}{36.46} E_{md},$$

so that $R_0 = 20$, $R = 36.46$

$$P(36.46, 20) = \frac{1}{1+\left(\frac{36.46}{20}\right)^2} = 0.231,$$

and interference exists for 23% of the hour.

4. Distribution of Interference from Night-to-Night.

A similar computation may be readily made with respect to the interference resultant from night-to-night fading. In this case, however, numerical methods must be applied to empirically tabulated probability functions and these are most readily available in the form of distributions.

Again the probability that undesired median field E_{mu} and the desired median field E_{md} lie in the element of area $dE_{mu}\, d\, E_{md}$ is taken to be

4.1 $$W(E_{mu}, E_{md}) = W(E_{mu}) W(E_{md})$$

subject to the assumption that $W(E_{mu})$ is independent of $W(E_{md})$

The assumption in this case is certainly an approximation. A statistical examination in some detail of fields received in the same hour on the same day in Atlanta and in Baltimore from WLW has shown that the correlation between the fields over two paths as close together as these even is remarkably low, and a

test use of the assumption in a case where a direct check was available showed fair argument. It is believed that the ass-umption will prove quite accurate for widely separated transmission paths.

The probability that E_{md} will exceed E_{mu} by a factor of R or larger can then be obtained by integrating

$$4.2 \qquad \int W(E_{mu})\, W(E_{md})\, d E_{mu}\, d E_{md}$$

$$= \int d P(E_{mu})\, d P(E_{md})$$

over the area that lies below the line $E_{md} = R E_{mu}$. Correspondingly, the probability that E_{md} exceeds E_{mu} by a factor of R or more and also remains above some specified level E_{mdo} is obtained by omitting the integration below E_{mdo}.

The numerical integration may be carried out in various ways. In the cases that have been computed, log-log coordinates have been used for E_{mu} and E_{md} so that the lines $E_{md} = R\, E_{mu}$ are parallel lines for various values of R. A P-P grid was superimposed with d P = 0.05 so that the equi-probability cells generated each had a value of $\frac{1}{4}\%$.

5. Distribution of the Instantaneous Amplitude of the Sum of a Groundwave and a Skywave.

The probability $W(\mathcal{E})$ by the procedure 2.2 must result from

$$5.1 \qquad W(\mathcal{E}_s) = \frac{1}{\pi E_o^2}\, e^{-\frac{E^2}{E_o^2}}$$

for the skywave and from

$$5.2 \qquad W(\mathcal{E}_g) = \frac{1}{2\pi E_g}\, \delta(E - E_g),$$

in which δ is the Dirac function, for the groundwave.

The transform of $w(\mathcal{E}_s)$ is (Cf. 2.4)

$$5.3 \qquad e^{-\frac{E_o^2}{4} p^2}$$

and that of $w(\mathcal{E}_g)$ is

$$5.4 \quad \frac{1}{2\pi E_g} \int_{space} e^{ir E \cos\theta} \, \delta(E - E_g) E \, dE \, d\theta = J_o(r E_g).$$

Then

$$5.5 \quad A(h) = J_o(r E_g) \, e^{-\frac{E_o^2}{4} r^2}$$

and

$$5.6 \quad W(\mathcal{E}) = \frac{1}{4\pi^2} \int_{space} e^{-r E \cos\theta} J_o(r E_g) \, e^{-\frac{E_o^2}{4} r^2} \, r \, dr \, d\theta$$

$$= \frac{1}{2\pi} \int_0^\infty J_o(rE) \, J_o(r E_g) \, e^{-\frac{E_o^2}{4} r^2} \, r \, dr$$

$$= \frac{1}{\pi E_o^2} e^{-\frac{E^2 + E_g^2}{E_o^2}} \, I_o\left(\frac{2 E E_g}{E_o^2}\right).$$

(Cf. Watson, Treatise on Bessel Functions, p 395).

The distribution is then determined by

$$5.7 \quad 1 - P(E) = \int_0^{2\pi} d\theta \int_0^E W(\mathcal{E}) \, E \, dE$$

$$= \int_0^E e^{-\frac{E^2 + E_g^2}{E_o^2}} \, I_o\left(\frac{2 E E_g}{E_o^2}\right) \frac{2E}{E_o^2} \, dE$$

Iterated partial integration of this expression determines almost immediately

$$5.8 \quad P(E) = 1 - e^{-\frac{E^2 + E_g^2}{E_o^2}} \sum_1^\infty \left(\frac{E}{E_g}\right)^n I_n\left(\frac{2 E E_g}{E_o^2}\right).$$

Fig.2.1

ANNUAL AVERAGE FIELD INTENSITIES

E_{ma} Values in SS+2; Number of Data in Parentheses

DISTANCE (Miles)	PATH	LATITUDE (Degrees)	AVERAGES UV/M 1939	1940	1941	1942	1943(2)	1944(2)	$E_{o\ .311\lambda}$ mv/m at 1 mile
96.2	B-WCAU	39.65	235 (240)		N	N	N	N	210
163	B-WABC	40.1		412 (295)	N	N	N	N	910
257	B-WHAM	41.2	N	N	731 (P) (64)	883 (82)	717 (82)	790 (85)	1185
268	G-WHO	41.3	563 (87)	548 (90)	637 (90)	862 (117)	753 (115)	915 (117)	1100
273	B-WPTF	37.57	140[a] (80)	215[a] (80)		157[b] (82)	150[b] (81)	190[b] (80)	492[a] 194[b]
343	G-KOA	40.4	774 (90)	898 (91)	658 (91)	978 (162)	1129 (164)	1023 (119)	1310
354	A-WCKY	36.5	1673[c] (136)	1650[c] (363)		N		2220[d] (330)	2020[c] 1414[d]
374	A-WLW	36.7		773[g] (365)	361[g] (346)		1111[h] (P) (265)	1114 (300)	1460[g] 1230[h]
387	G-KSTP	43.0	N	N	N			1183) 1104) (121)	1819
390	G-WCCO	43.0	213 (83)	256 (91)	293 (92)	510 (111)	365 (120)	586 (122)	1520
413	B-WLW	39.4		397[i] (360)	347 (349)	692[j] (357)	649 (335)	900[j] (336)	1540[i] 1300[j]
430	B-WCKY	39.25	N	608[e] (320)		963[f] (340)	803[f] (330)	1220[f] (290)	2420[e] 1515[f]
558	G-WFAA	36.9	897 (90)	995 (91)	878 (91)	1104 (316)	1314 (310)	1140 (125)	1660
712	G-KSL	41.0	609 (92)	739 (90)	565 (89)	785 (170)	896 (118)	N	1615

(continued)

N indicates no recordings made; P =recordings for over 3/4 of year; blanks =less than 3/4 year.

(1) Estimated from SS+5 data and Median Diurnal Curve. Figure 2.5

(2) These averages have been corrected for the 1 db wartime power reduction.

FIGURE 2.1

Fig. 2.1 (continued)

DISTANCE (Miles)	PATH	LATITUDE (Degrees)	AVERAGES UV/M 1939	1940	1941	1942	1943 (2)	1944 (2)	E_{o},311Å mv/m at 1 mile
752	G-WLW	40.35	189[k] (88)	267[k] (92)	167[k] (88)	194[ℓ] (310)	278[ℓ] (301)	355[ℓ] (121)	1840[k] 1550[ℓ]
783	G-WOAI	35.23	689 (91)	709 (91)	604 (91)	607 (319)	605 (306)	616 (122)	1660
884	P-CBK	48.8	N	N	N	140 (P) (185)	79.7 (76)	236 (74)	1770
1176	G-KFI	39.5	N	N	115 (93)	185 (114)	207 (116)	146 (120)	1550
1192	G-KNX	38.0	134 (89)	138 (66)	N				1725
1220	B-WFAA	38.1	84.2 (82)	113 (86)	120 (90)	150 145 (8[r])	208 198 (72)	182 180 (72)	1770
1424	P-KSTP	46.1	N	N	N		29.4 (70)	75.8 (92)	2620
1438	P-WCCO	46.2	N	N	N		18.6 17.3 (75)	48.7 45.0 (90)	1770
1607	P-WFAA	42.9	30.3 29.3 (86)	33.1 30.8 (86)	70.2 67.5 (77)	13.1 12.6 (85)	49.0 48.3 (82)	82.3 80.90 (89)	1770
1731	P-WENR	45.45	7.23 6.50 (80)	15.8 11.6 (87)	23.4 18.8 (83)	39.0 25.2 (84)	20.5 15.6 (78)	36.2 28.9 (81)	1730
1973	P-WLW	45.1	11.3[m] 9.6 (70)	11.63[m] 9.78 (82)	17.6[m] 16.0 (84)	33.6[n] 26.7 (49)	15.2[n] 10.6 (60)	30.1[n] 23.9 86)	1910[m] 1610

(continued)

. . . . . .

FIGURE 2.1

Fig. 2.1 (continued 2)

DISTANCES (Miles)	PATH	LATITUDE (Degrees)	AVERAGES UV/M 1939	1940	1941	1942	1943(2)	1944(2)	E_{o} .311λ mv/m at 1 mile
2041	P-WWL	42.5	N	N	N		68.9 66.1 (72)	99.2 94.4 (84)	2350
2163	P-WSB	43.8	6.76 5.53 (74)	7.06 5.58 (78)	17.6 14.4 (83)	18.9 13.8 (53)	18.9 12.0 (72)	27.4 20.7 (88)	1660
2308	B-KFI	39.4	13.9 12.0 (69)	19.2 14.6 (50)	N	N	N	N	1480
2326	B-KNX	39.5	21.6(1) est.	23.7(1) est.	N	N	N	N	1732
2411	P-WABC	46.1	N	N	N	5.48 3.18 (158)	3.2 1.1 (181)	N	1500
2446	B-KPO	40.5	18.4(1) est.	21.3(1) est.		N	N	N	1130

.....End or Fig. 2.1

FIGURE 2.1

Fig. 2.2

DISTRIBUTIONS OF NIGHT TO NIGHT MEDIAN FIELDS IN SS+2 HOUR WITH RESPECT TO THEIR ANNUAL AVERAGES AS A UNIT

LAT.	PATH	DIST.	FREQ.	$R = E_{mp} / E_{ma}$											No. OF DATA
				$P_c(R)=5$	10	20	30	40	50	60	70	80	90	95	
35.2	G-WOAI	783	1200	1.82	1585	1.89	1.26	1.06	0.97	0.885	.800	.708	.585	.480	896
36.5	A-WCKY	354	1530	1.79	1.61	1.37	1.21	1.10	0.98	.862	.745	.822	.477	.342	336*
36.7	A-WLW	374	700	2.20	1,98	1,63	1.36	1.11	.925	.755	.578	.376	.185	.105	299
36.9	G-WFAA	558	820	1.90	1.69	1.45	1.28	1.13	.990	.850	.700	.516	.295	.151	1023
39.25	B-WCKY	430	1530	1.92	1.68	1.41	1.23	1.09	.980	.865	.735	.555	.290	.120	291
39.4	B-WLW	413	700	2.70	2.14	1.66	1.35	1.05	.800	.545	.333	.183	.092		1034
39.5	G-KFI	1176	640	2.10	1.75	1.44	1.23	1.07	.910	.770	.635	.515	.348	.225	432
39.55	G-KNX	1192	1070	2.14	1.73	1.38	1.19	1.05	.920	.790	.665	.547	.410	.305	152
40.35	G-WLW	752	700	3.40	2.61	1.72	1.25	.920	.675	.487	.335	.211	.108		729
40.4	G-KOA	343	850	2.38	2.00	1.54	1.27	1.06	.870	.692	.517	.335	.157		717
41.0	G-KSL	712	1160	2.45	1.98	1.50	1.26	1.07	1895	.708	.520	.320	.103		441
41.3	G-WHO	268	1040	2.67	2.18	1.62	1.27	1.00	.781	.593	.410	.208			613
42.9	P-WFAA	1607	820	2.80	2.20	1.63	1.31	1.02	.735	.500	.328	.200	.100		312
43.0	G-WCCO	390	850	3.20	2.40	1.72	1.32	.950	.660	.417	.237	.125			616
43.6	G-KSTP	387	1500	2.47	1.97	1.55	1.31	1.07	.857	.648	.455	.253			121
43.8	P-WSB	2163	750	5.55	3.41	1.46	.948	.632	.429	.293	.200	.133			364
45.45	P-WENR	1731	890	4.22	2.70	1.44	.905	.604	.420	.290	.189	.108			407
46.2	P-WCCO	1438	930	3.40	2.48	1.60	1098	.742	.530	.387	.263	.161			151
48.4	P-CBK	884	540	3.45	2.37	1.54	1.14	.840	.610	.438	.305	.200	.119		305

* +3 Hour taken instead of +2 Hour.

FIGURE 2.2

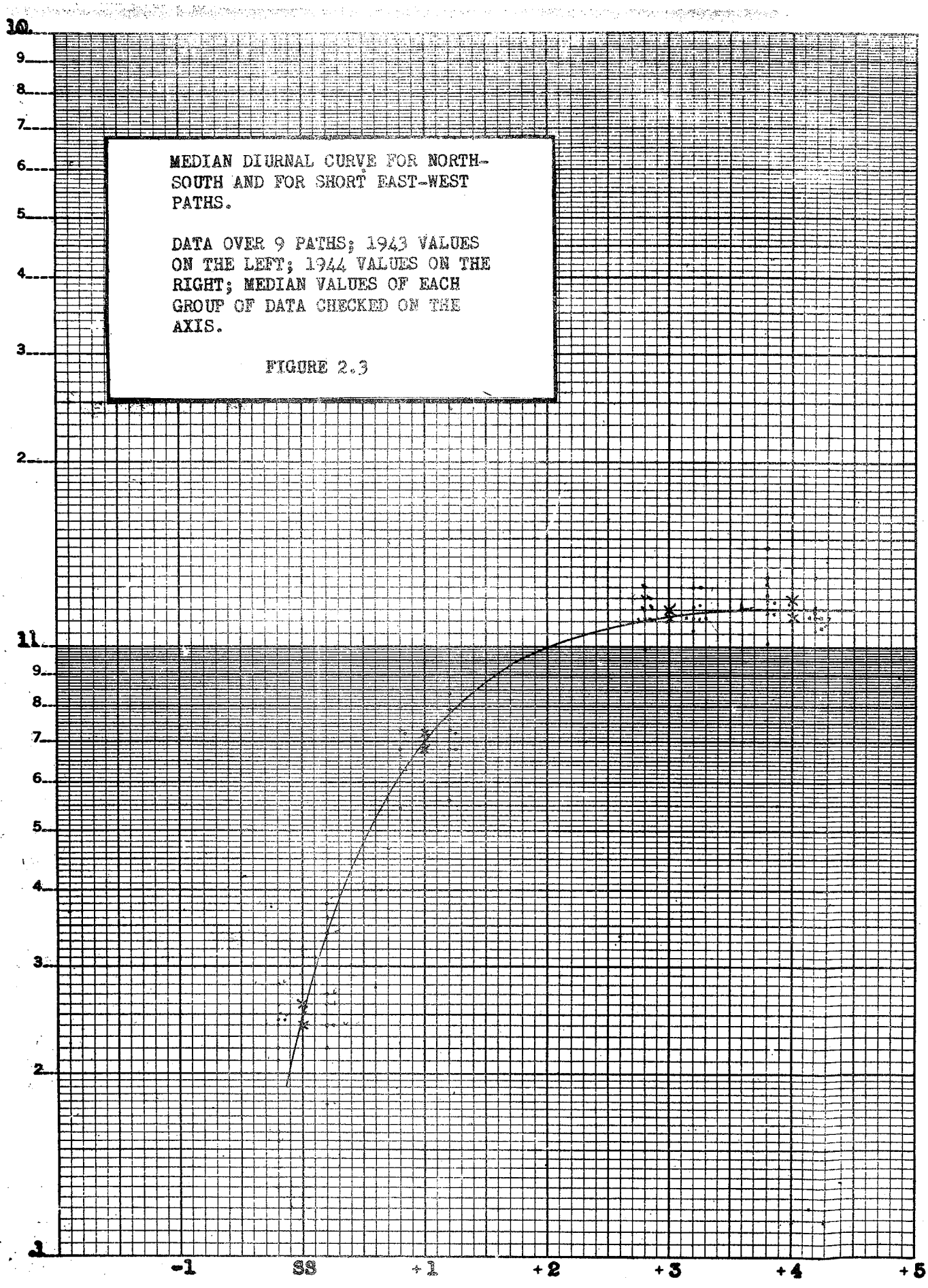
MEDIAN DIURNAL CURVE FOR NORTH-SOUTH AND FOR SHORT EAST-WEST PATHS.
DATA OVER 9 PATHS; 1943 VALUES ON THE LEFT; 1944 VALUES ON THE RIGHT; MEDIAN VALUES OF EACH GROUP OF DATA CHECKED ON THE AXIS.
FIGURE 2.3
10
9
8
7
6
5
4
3
2
11
9
8
7
6
5
4
3
2
1
-1
SS
+1
+2
+3
+4
+5
KEUFFEL & ESSER CO., N. Y. 359-510
Semi-Logarithmic 2 cycles × 10 to the inch, 5th lines accented.
MADE IN U.S.A.

FIGURE 2.3

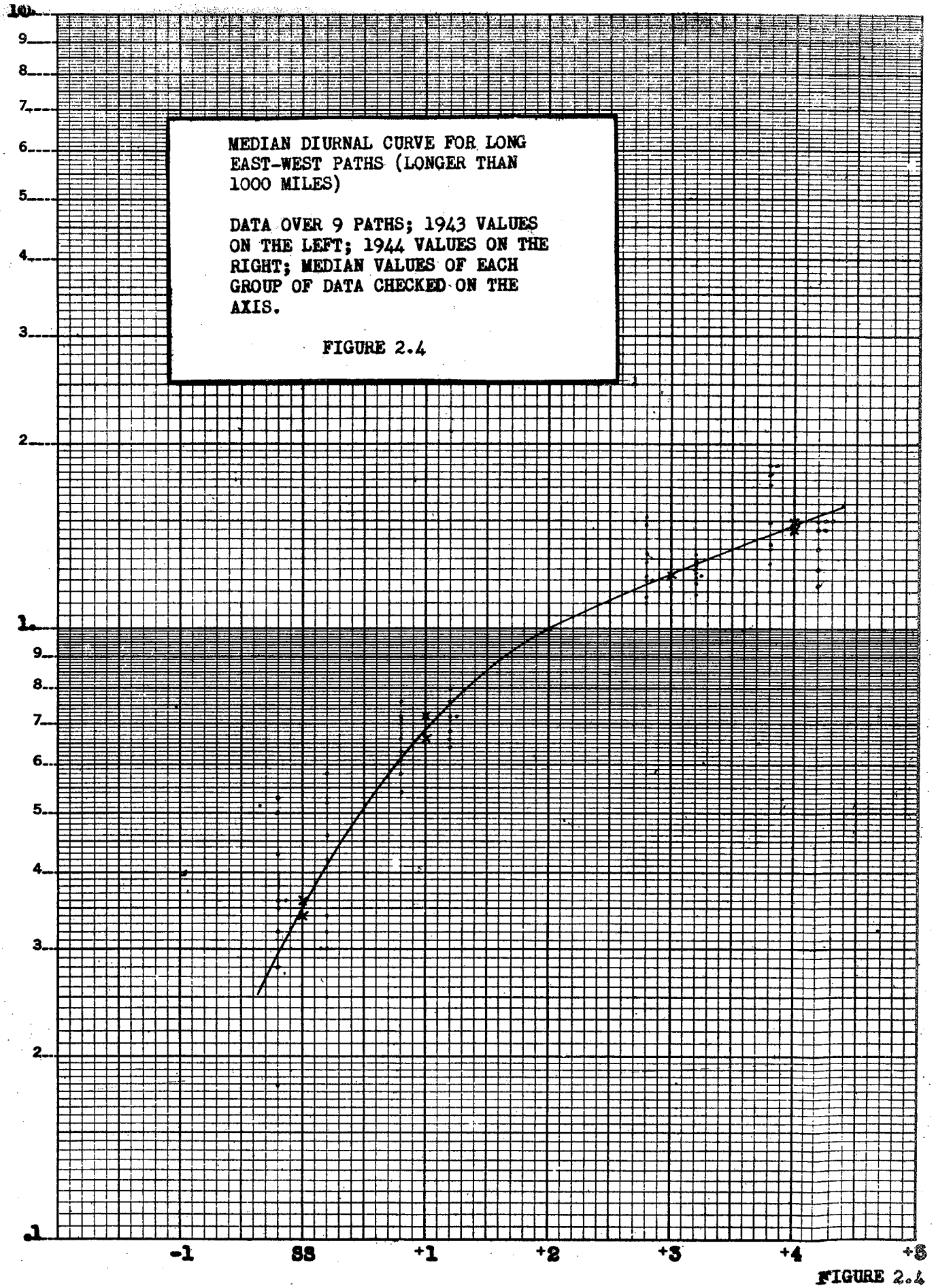

MEDIAN DIURNAL CURVE FOR LONG EAST-WEST PATHS (LONGER THAN 1000 MILES)

DATA OVER 9 PATHS; 1943 VALUES ON THE LEFT; 1944 VALUES ON THE RIGHT; MEDIAN VALUES OF EACH GROUP OF DATA CHECKED ON THE AXIS.

FIGURE 2.4

KEUFFEL & ESSER CO., N. Y. 359-816
Semi-Logarithmic 2 cycles X 10 to the inch, 5th lines accented.
MADE IN U. S. A.

FIGURE 2.4

Fig. 2.5

MEDIAN DIURNAL CURVE DATA

RATIOS OF FIELDS IN VARIOUS NIGHT-TIME HOURS TO THOSE IN SS+2

PATH	DISTANCE	S S		+ 1		+ 2		+ 3		+ 4	
		43	44	43	44	43	44	43	44	43	44
(1) LONG EAST-WEST PATHS (longer than 1,000 miles) :--											
P-WSB	2163	.34	.32	.64	.72	1.	1.	1.32	1.11	1.50	1.15
P-WWL	2041	.30	.27	.71	.70	1.	1.	1.21	1.12	1.35	1.17
P-WLW	1973	.32	.36	.66	.63	1.	1.	1.26	1.33	1.45	1.85
P-WENR	1731	.46	.36	.72	.58	1.	1.	1.23	1.52	1.46	1.85
P-WFAA	1607	.30	.18	.70	.54	1.	1.	1.18	1.28	1.25	1.38
P-WCCO	1438	.25	.35	.68	.62	1.	1.	1.25	1.48	1.50	1.72
P-KSTP	1424	.58	.50	.80	.71	1.	1.	1.13	1.22	1.17	1.36
B-WFAA	1220	.42	.53	.74	.76	1.	1.	1.22	1.22	1.50	1.50
G-KFI	1176	.52	.43	.72	.66	1.	1.	1.29	1.23	1.45	1.27
(2) NORTH -SOUTH and SHORT EAST -WEST PATHS :--											
G-WOAI	783	.24	.21	.79	.76	1.	1.	1.11	1.15	1.12	1.21
G-WFAA	558	.24	.16	.68	.63	1.	1.	1.11	1.20	1.07	1.30
B-WCKY	430	--	.22	--	.73	--	1.	--	1.20	--	1.27
B-WLW	413	.22	--	.64	--	1.	--	1.25	--	1.145	--
G-WCCO	390	.26	.24	.72	.68	1.	1.	1.116	1.12	1.126	1.128
G-KSTP	387	.36	--	.84	--	1.	--	--	1.06	--	1.06
A-WLW	374	.178	.155	.56	.545	1.	1.	1.25	1.25	1.30	1.45
A-WCKY	354	--	.26	--	.80	--	1.	--	.99	--	1.01
G-KOA	343	.34	.245	.68	.66	1.	1.	1.115	1.115	1.125	1.180
G-WHO	268	.38	.28	.76	.72	1.	1.	1.17	1.16	1.16	1.18
B-WHAM	257	.27	.245	.73	.63	1.	1.	1.12	1.12	1.125	1.127

FIGURE 2.5

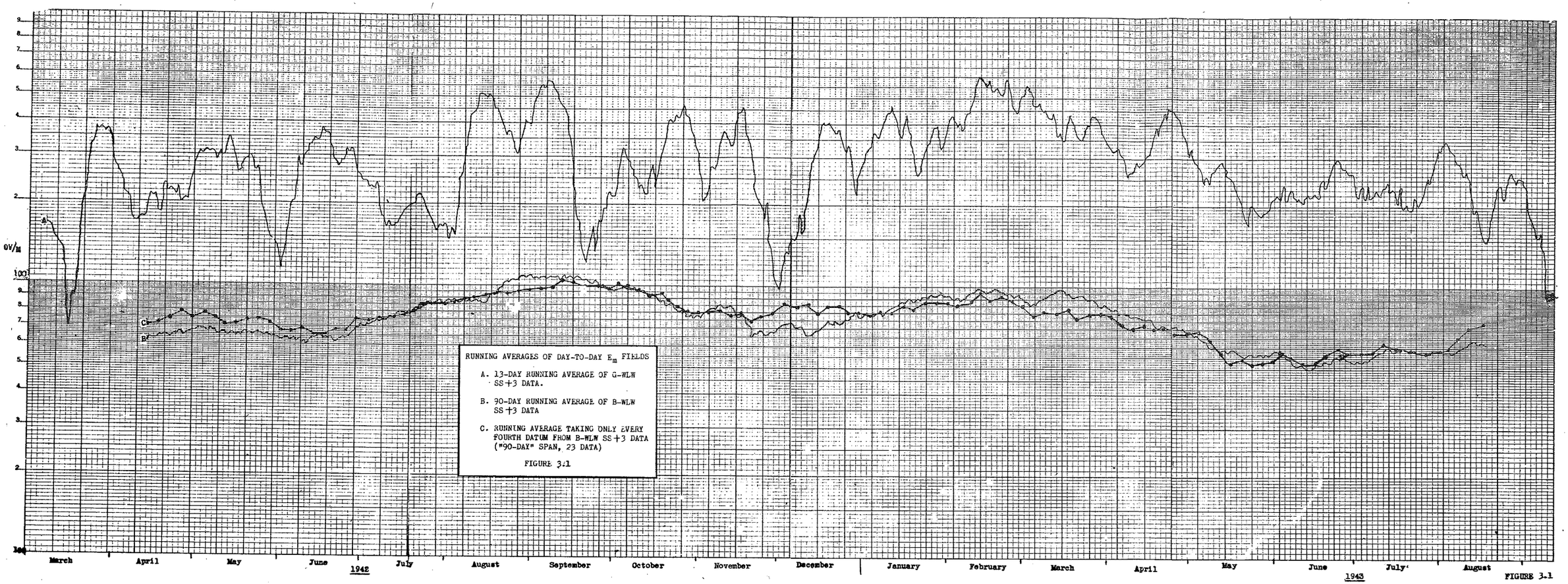

RUNNING AVERAGES OF DAY-TO-DAY E_m FIELDS

A. 13-DAY RUNNING AVERAGE OF G-WLW SS+3 DATA.

B. 90-DAY RUNNING AVERAGE OF B-WLW SS+3 DATA

C. RUNNING AVERAGE TAKING ONLY EVERY FOURTH DATUM FROM B-WLW SS+3 DATA ("90-DAY" SPAN, 23 DATA)

FIGURE 3.1

FIGURE 3.1

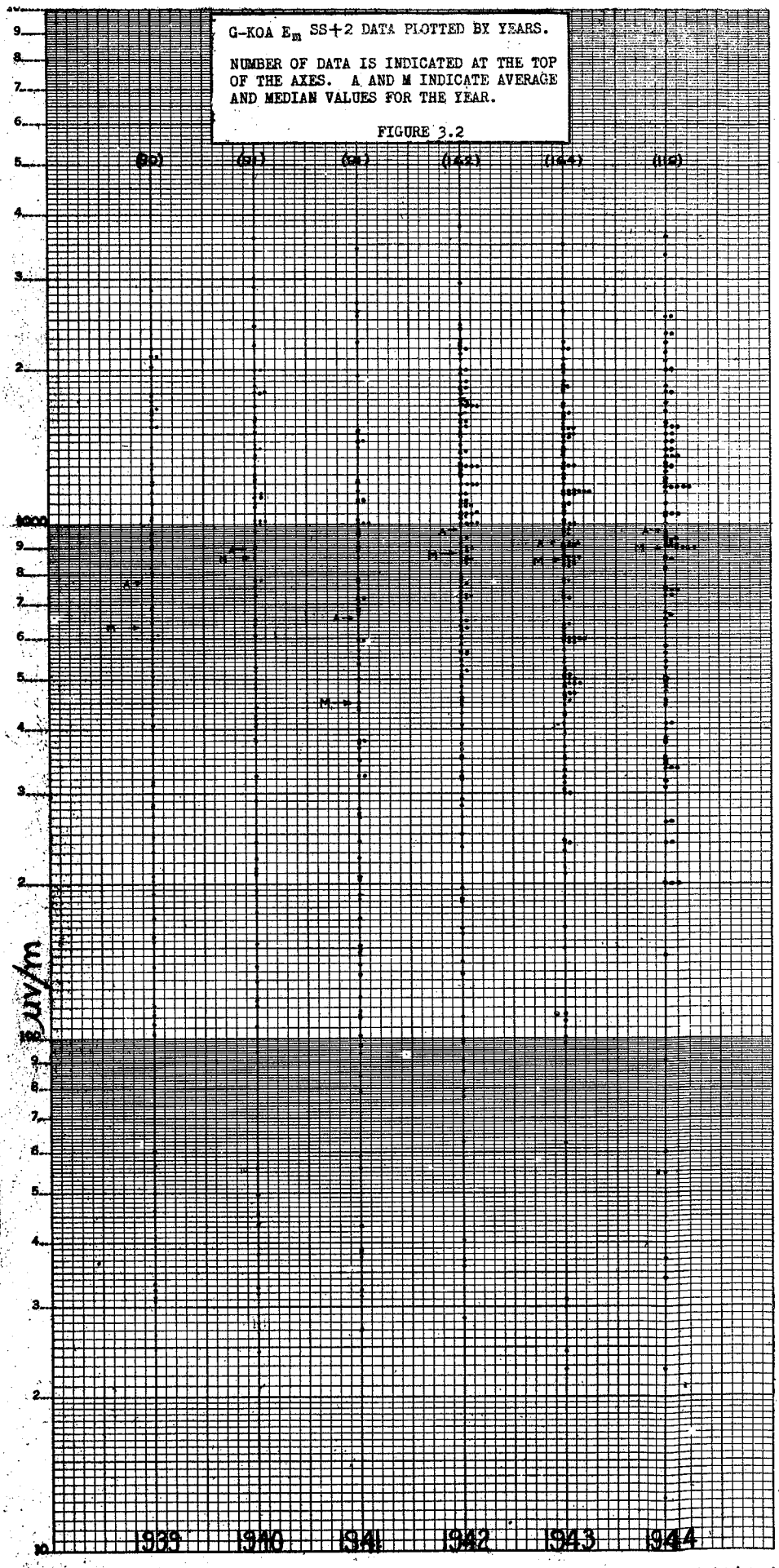
G-KOA E_m SS+2 DATA PLOTTED BY YEARS.
NUMBER OF DATA IS INDICATED AT THE TOP OF THE AXES. A AND M INDICATE AVERAGE AND MEDIAN VALUES FOR THE YEAR.
FIGURE 3.2
(90)
(91)
(98)
(142)
(144)
(110)
μV/m
1939
1940
1941
1942
1943
1944

FIGURE 3.2

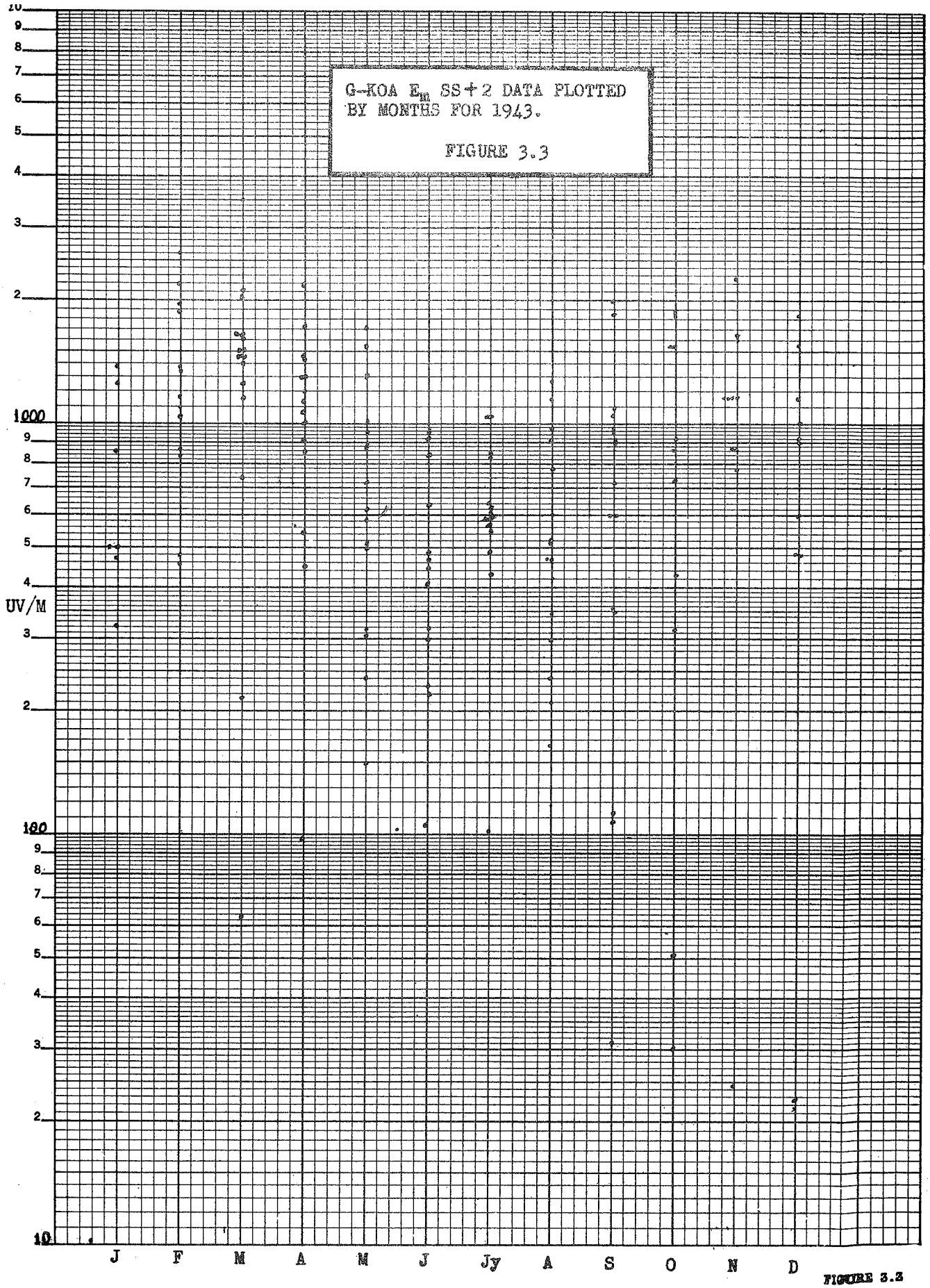
G-KOA E_m SS + 2 DATA PLOTTED BY MONTHS FOR 1943.
FIGURE 3.3
10
9
8
7
6
5
4
3
2
1000
9
8
7
6
5
4
UV/M
3
2
100
9
8
7
6
5
4
3
2
10
J
F
M
A
M
J
Jy
A
S
O
N
D

FIGURE 3.3

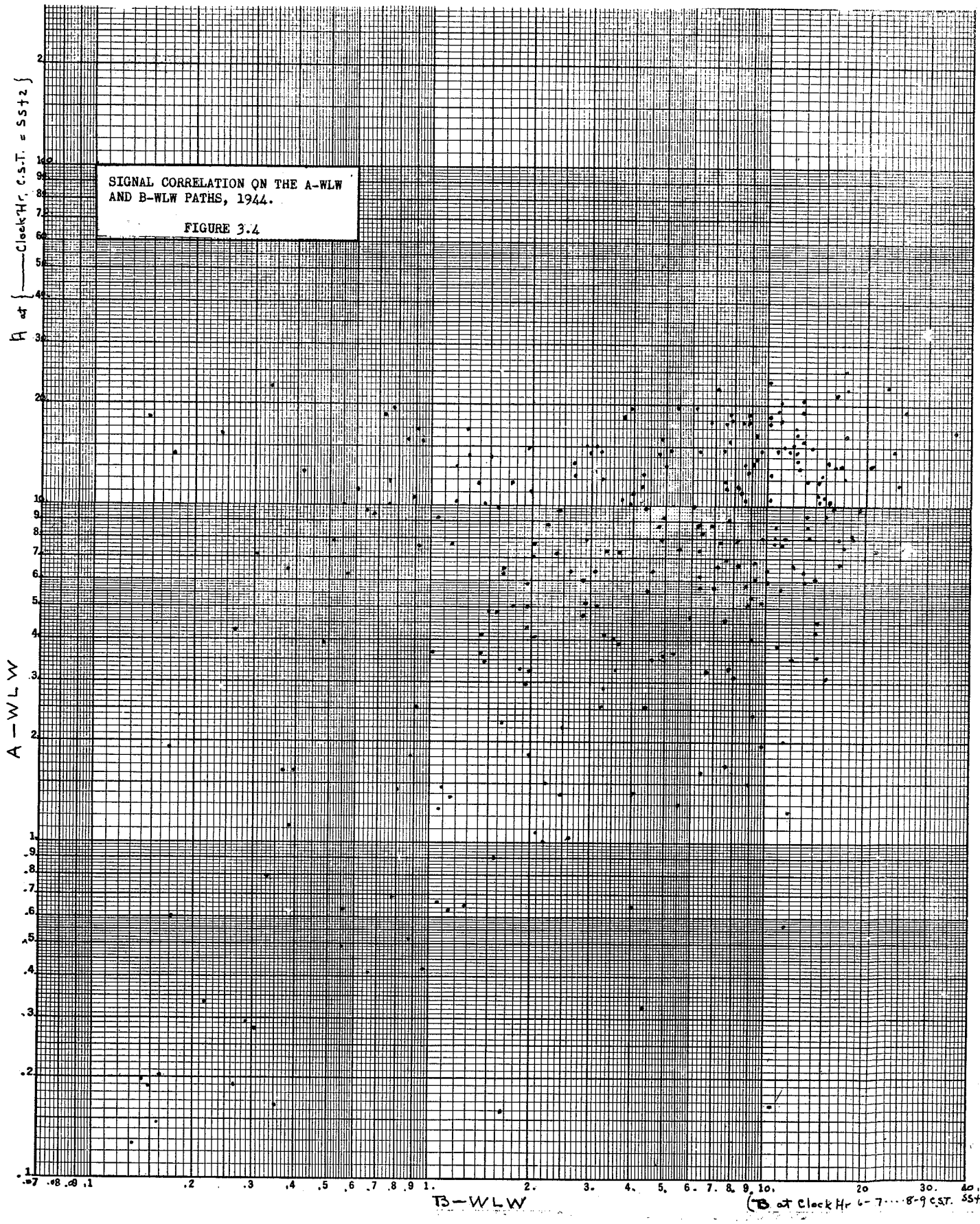

SIGNAL CORRELATION ON THE A-WLW AND B-WLW PATHS, 1944.

FIGURE 3.4

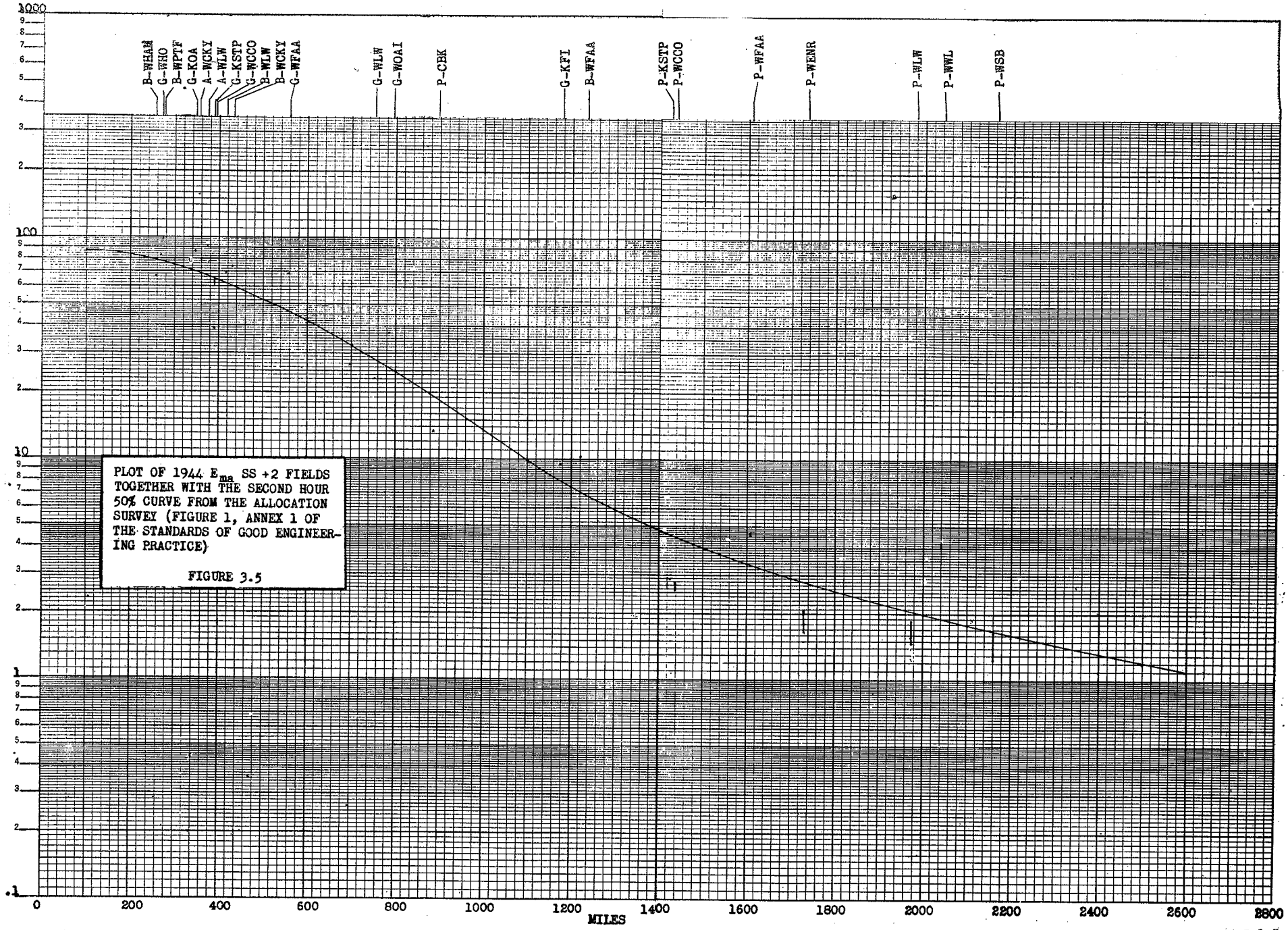

PLOT OF 1944 E_{ma} SS +2 FIELDS TOGETHER WITH THE SECOND HOUR 50% CURVE FROM THE ALLOCATION SURVEY (FIGURE 1, ANNEX 1 OF THE STANDARDS OF GOOD ENGINEERING PRACTICE)

FIGURE 3.5

FIGURE 3.5

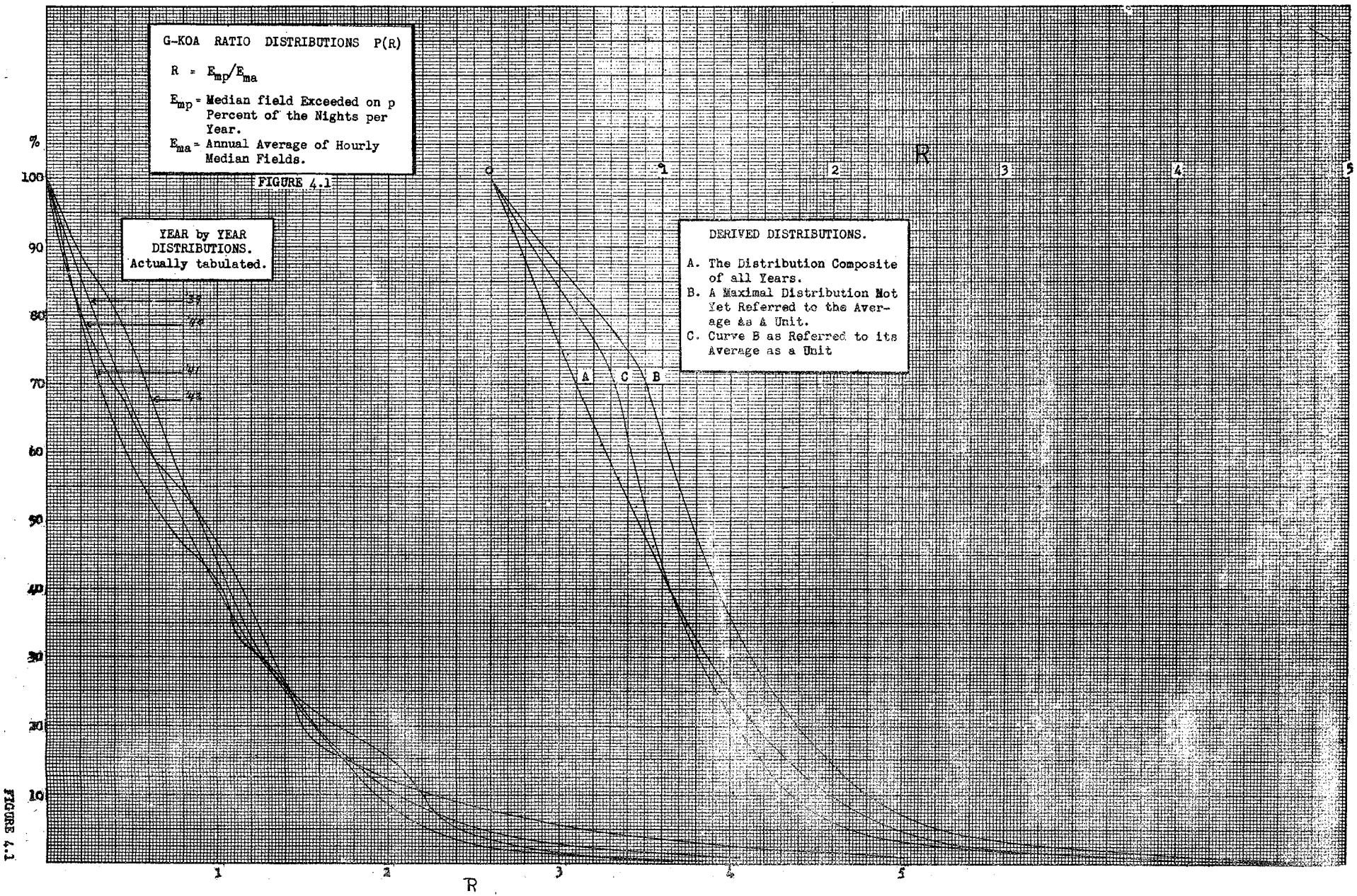
G-KOA RATIO DISTRIBUTIONS P(R)
R = E_{mp}/E_{ma}
E_{mp} = Median field Exceeded on p Percent of the Nights per Year.
E_{ma} = Annual Average of Hourly Median Fields.
FIGURE 4.1
YEAR by YEAR DISTRIBUTIONS. Actually tabulated.
DERIVED DISTRIBUTIONS.
A. The Distribution Composite of all Years.
B. A Maximal Distribution Not Yet Referred to the Average as A Unit.
C. Curve B as Referred to its Average as a Unit
%
R
A
C
B

FIGURE 4.1

EFFECT OF LATITUDE ON THE NIGHT-TO-NIGHT DISTRIBUTION OF MEDIAN FIELD INTENSITIES

$$R = \frac{E_{mp}}{E_{ma}}$$ where

E_{mp} = Median Field Exceeded on p Percent of the Nights per Year.

E_{ma} = Annual Average of Median Fields

P = Percent of the Nights per Year

FIGURE 5.1

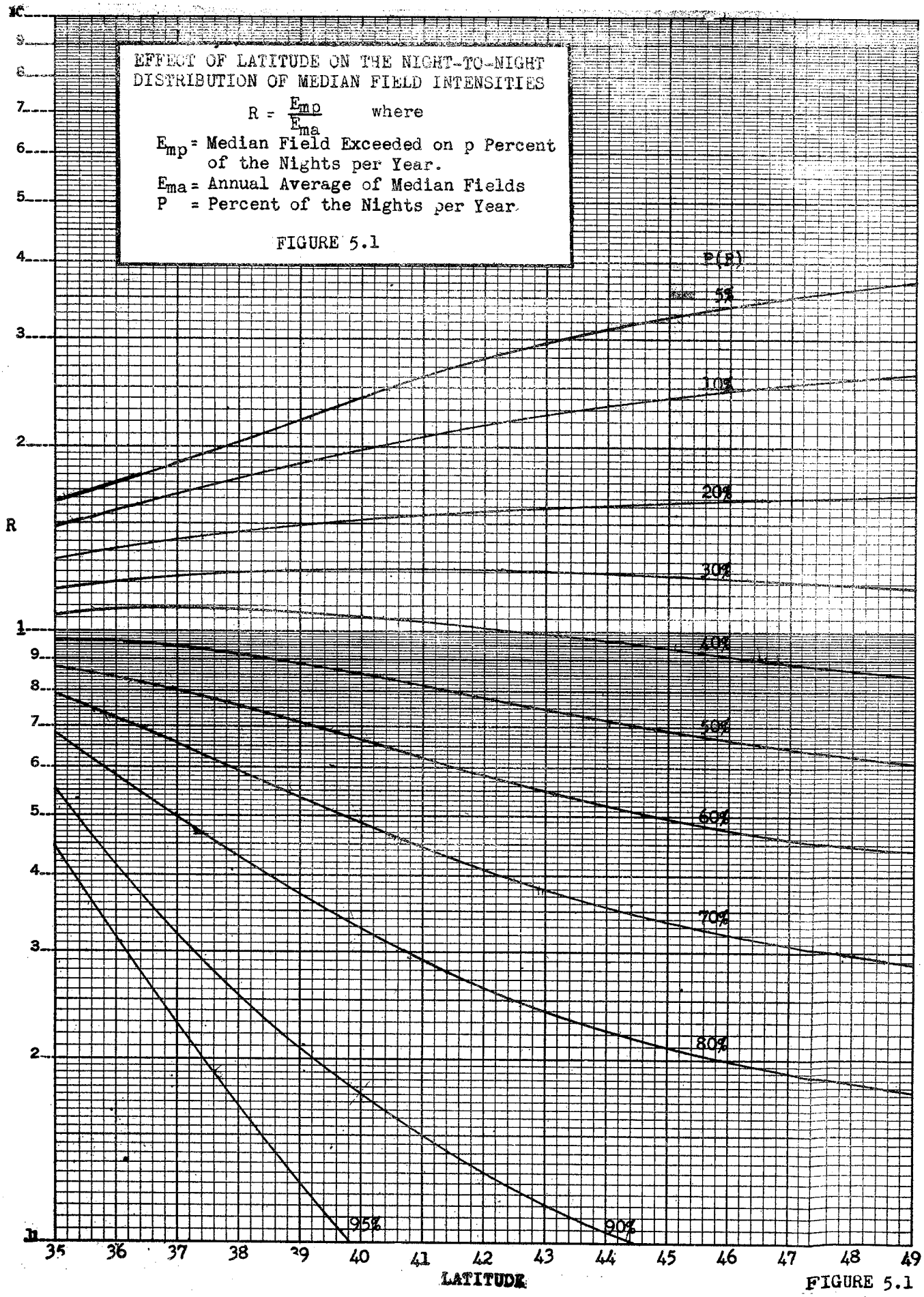

FIGURE 5.1

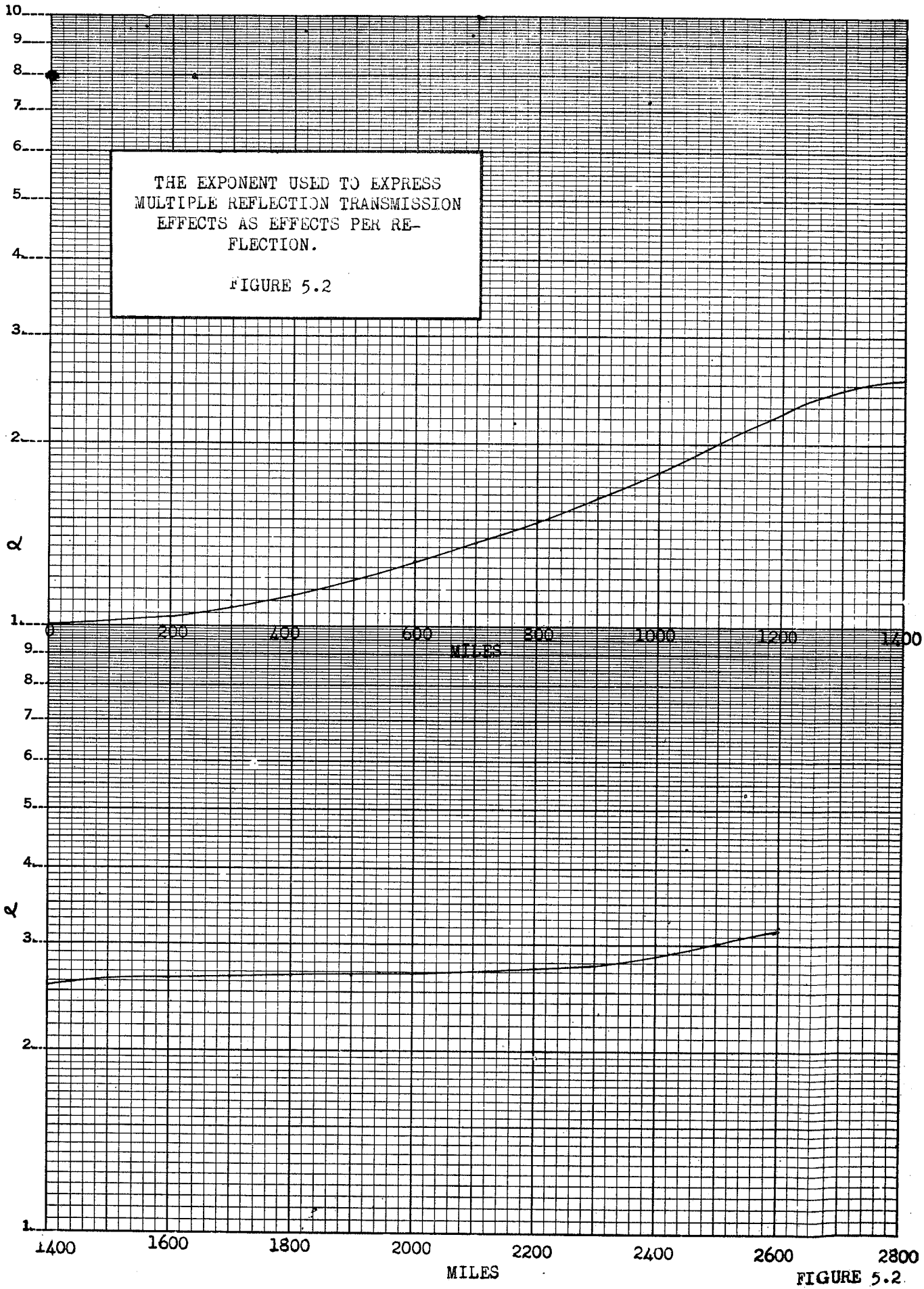
THE EXPONENT USED TO EXPRESS MULTIPLE REFLECTION TRANSMISSION EFFECTS AS EFFECTS PER RE-FLECTION.
FIGURE 5.2
α
MILES
0
200
400
600
800
1000
1200
1400
1600
1800
2000
2200
2400
2600
2800

FIGURE 5.2

DEVIATIONS PER REFLECTION
OF 1944 ANNUAL AVERAGES OF MEDIAN FIELDS FROM
THE SECOND HOUR 50% CURVE OF THE ALLOCATION SURVEY

FIGURE 5.3

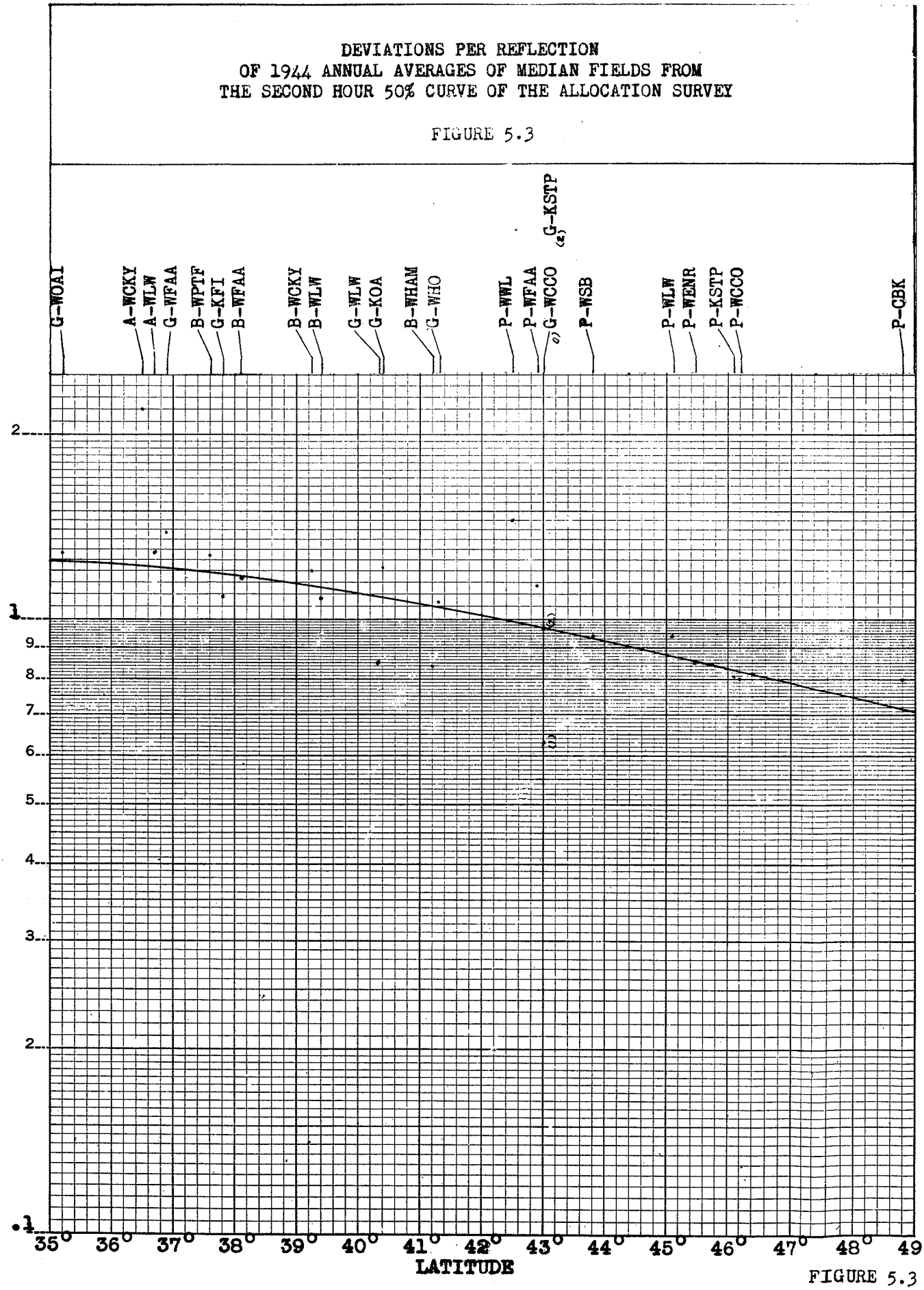

FIGURE 5.3

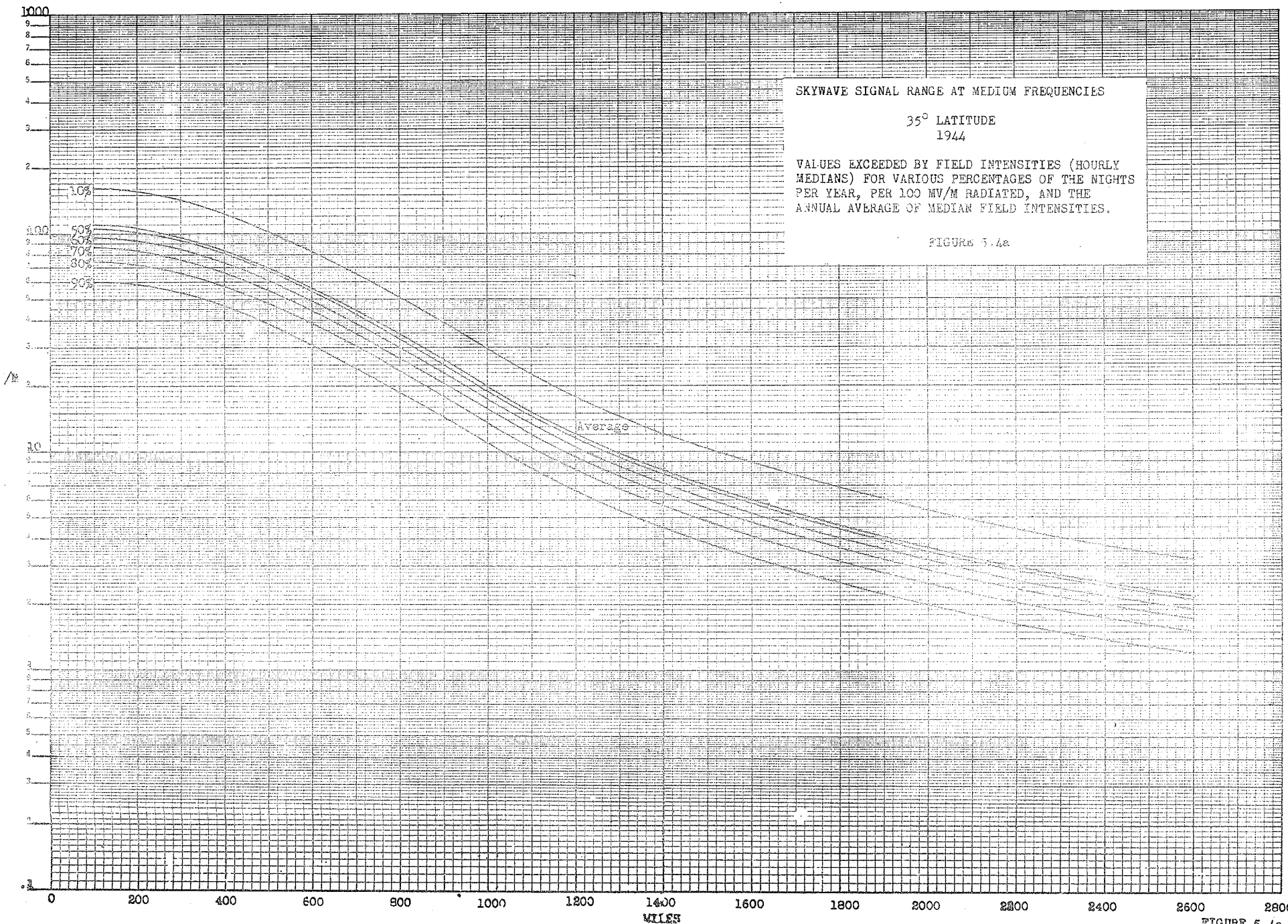
SKYWAVE SIGNAL RANGE AT MEDIUM FREQUENCIES
35° LATITUDE
1944
VALUES EXCEEDED BY FIELD INTENSITIES (HOURLY MEDIANS) FOR VARIOUS PERCENTAGES OF THE NIGHTS PER YEAR, PER 100 MV/M RADIATED, AND THE ANNUAL AVERAGE OF MEDIAN FIELD INTENSITIES.
FIGURE 5.4a
1000
100
10
1
/E
10%
50%
30%
70%
90%
Average
0
200
400
600
800
1000
1200
1400
1600
1800
2000
2200
2400
2600
2800
MILES
FIGURE 5.4a

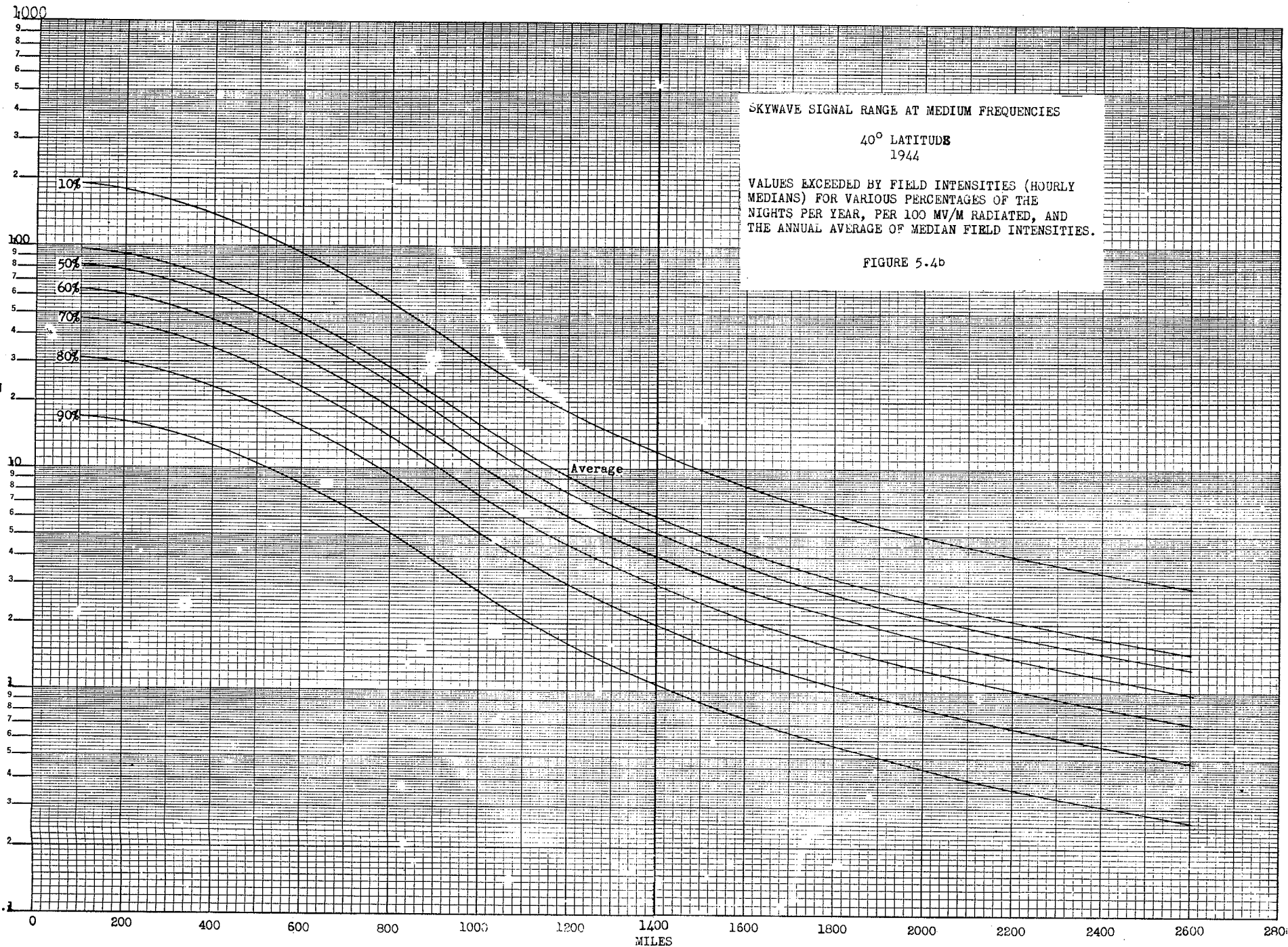
SKYWAVE SIGNAL RANGE AT MEDIUM FREQUENCIES
40° LATITUDE
1944
VALUES EXCEEDED BY FIELD INTENSITIES (HOURLY MEDIANS) FOR VARIOUS PERCENTAGES OF THE NIGHTS PER YEAR, PER 100 MV/M RADIATED, AND THE ANNUAL AVERAGE OF MEDIAN FIELD INTENSITIES.
FIGURE 5.4b
1000
100
10
1
MV/M
10%
50%
60%
70%
80%
90%
Average
0
200
400
600
800
1000
1200
1400
1600
1800
2000
2200
2400
2600
MILES

FIGURE 5.4b

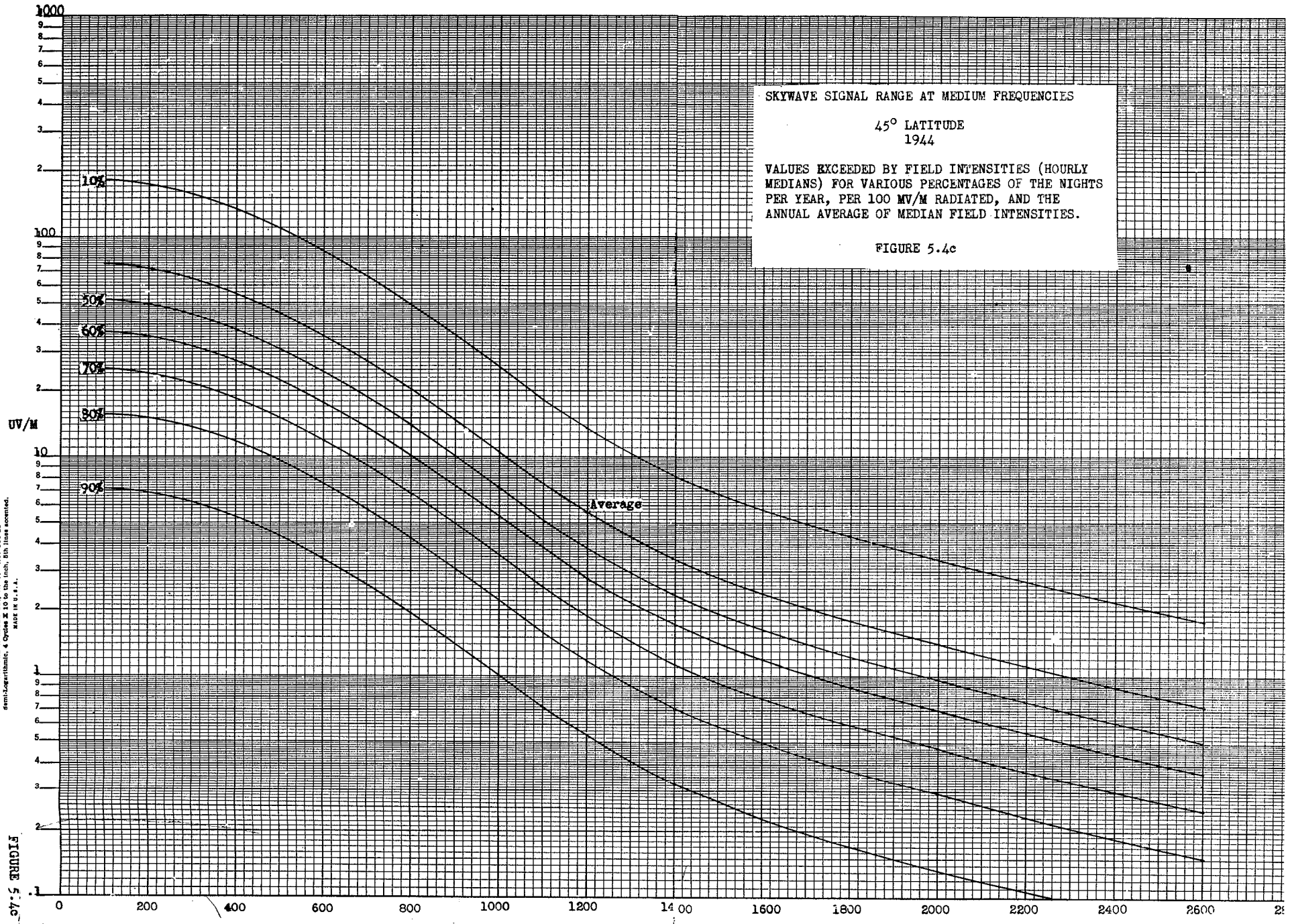
SKYWAVE SIGNAL RANGE AT MEDIUM FREQUENCIES
45° LATITUDE
1944
VALUES EXCEEDED BY FIELD INTENSITIES (HOURLY MEDIANS) FOR VARIOUS PERCENTAGES OF THE NIGHTS PER YEAR, PER 100 MV/M RADIATED, AND THE ANNUAL AVERAGE OF MEDIAN FIELD INTENSITIES.
FIGURE 5.4c
10%
50%
60%
70%
80%
90%
Average
UV/M
1000
100
10
1
0
200
400
600
800
1000
1200
1400
1600
1800
2000
2200
2400
2600

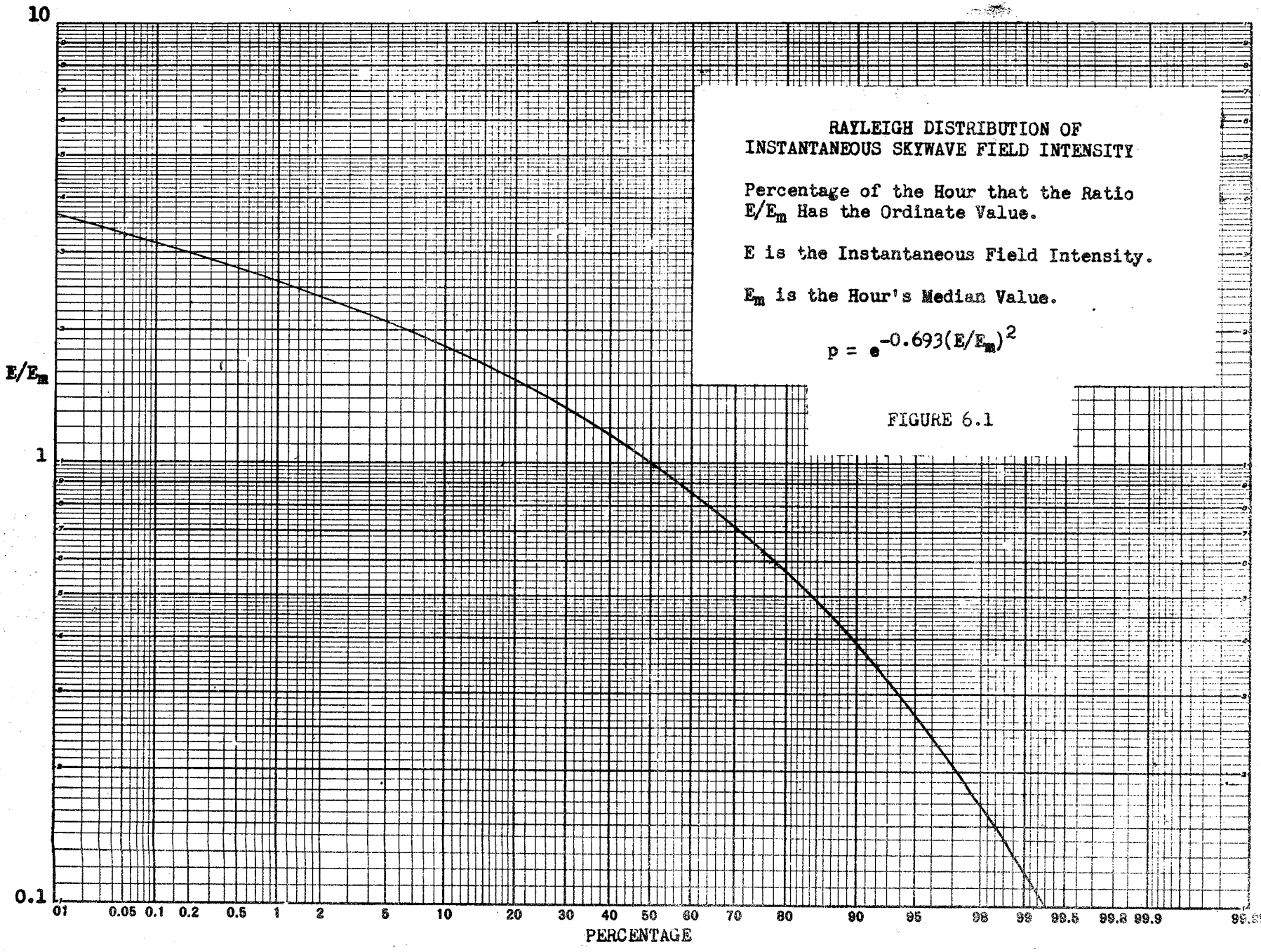
RAYLEIGH DISTRIBUTION OF
INSTANTANEOUS SKYWAVE FIELD INTENSITY
Percentage of the Hour that the Ratio
E/Em Has the Ordinate Value.
E is the Instantaneous Field Intensity.
Em is the Hour's Median Value.
p = e^-0.693(E/Em)^2
FIGURE 6.1
10
1
0.1
E/Em
0.01
0.05
0.1
0.2
0.5
1
2
5
10
20
30
40
50
60
70
80
90
95
98
99
99.5
99.8
99.9
99.99
PERCENTAGE

FIGURE 6.1

INTERFERENCE WITHIN THE HOUR

R_o is the Steady Signal Desired to Undesired Ratio Taken as Standard for Unobjectionable Interference.

$\tilde{R}$ is the Ratio of the Median Value of the Desired Skywave to that of the Undesired Skywave.

FIGURE 6.2

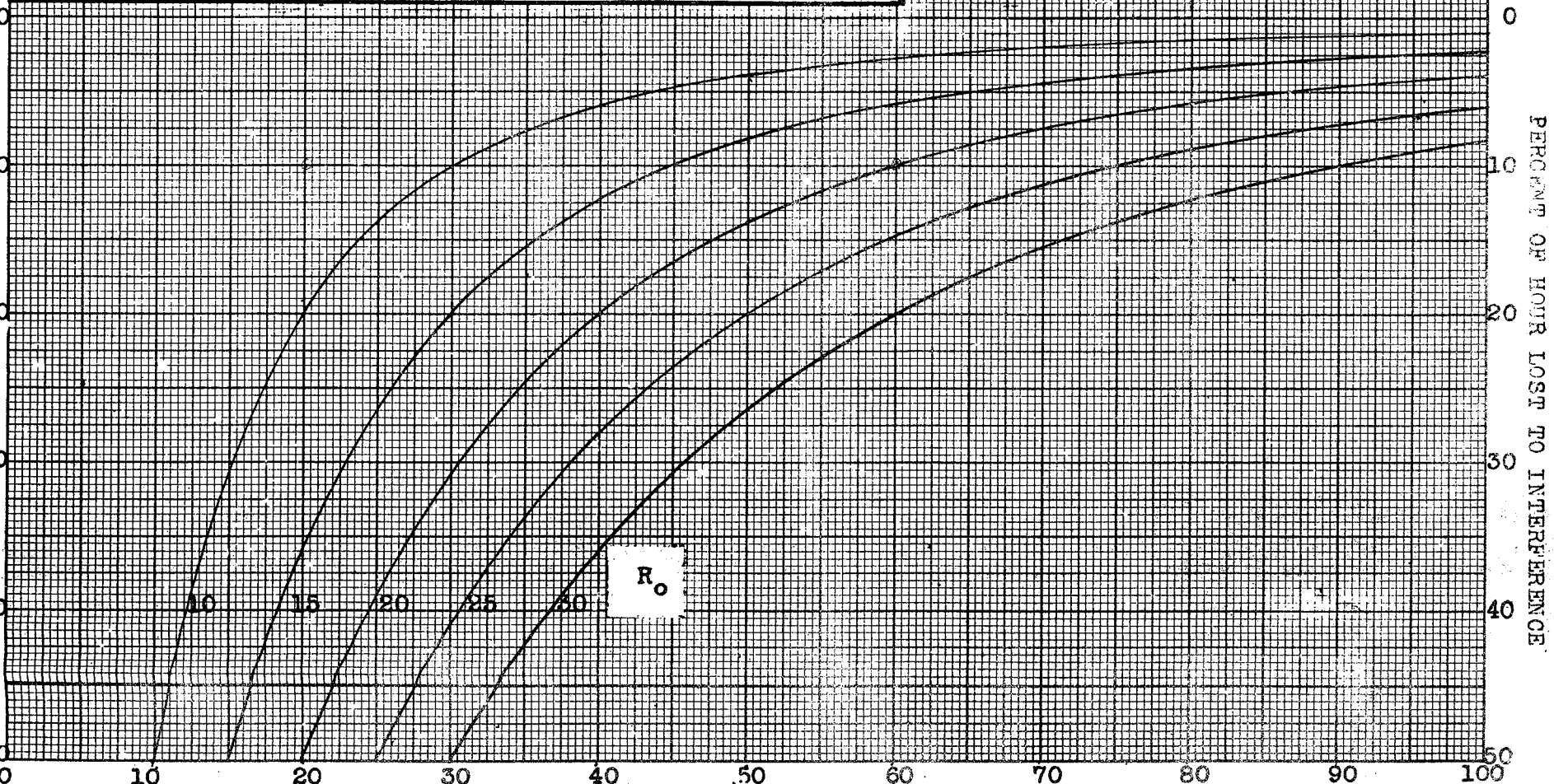

EFFECT OF NIGHT-TO-NIGHT FADING ON INTERFERENCE

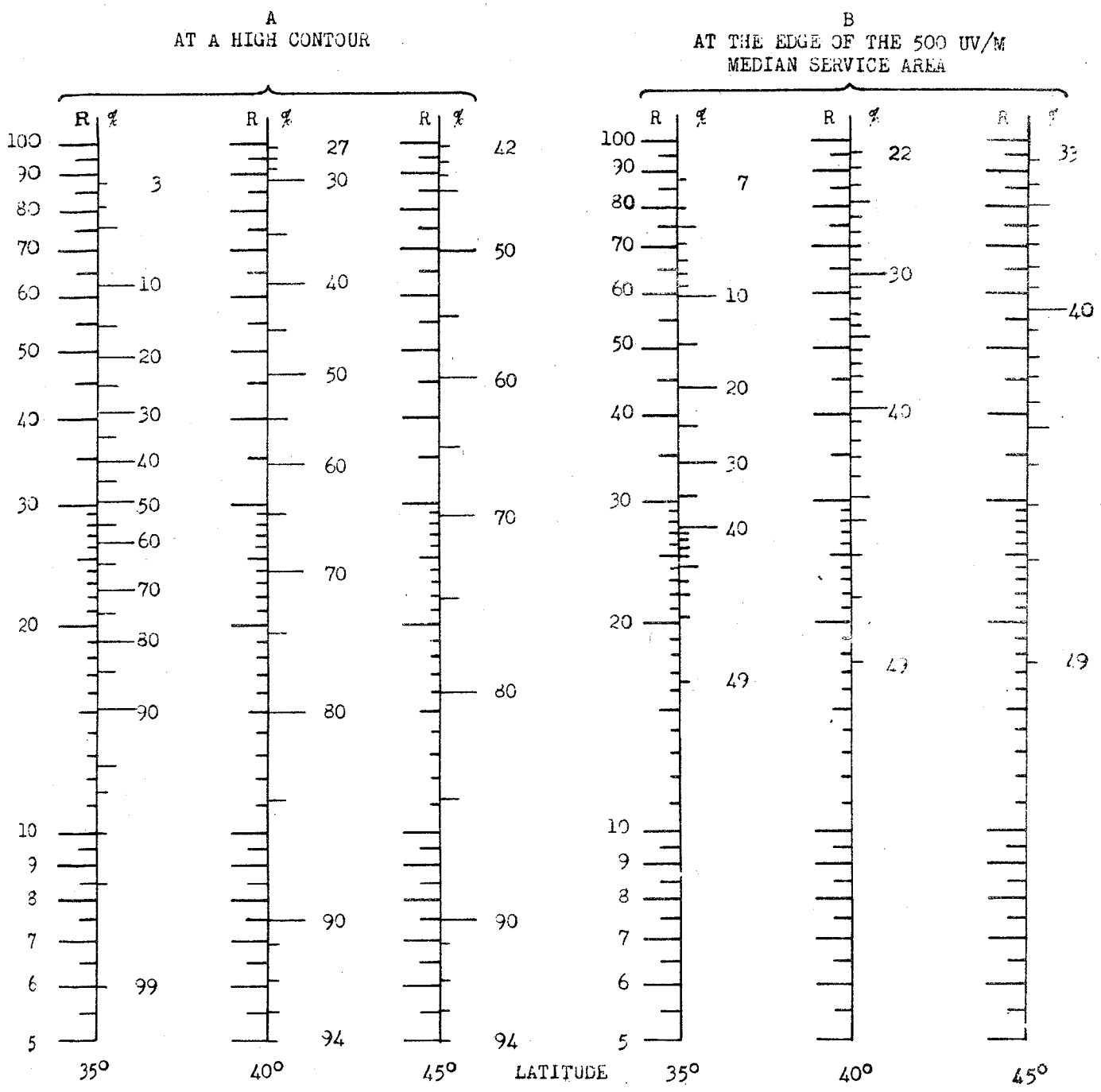

A THESE FUNCTIONS SHOW THE NUMBER OF NIGHTS PER YEAR (%) ON WHICH THE RATIO (R) OF THE DESIRED TO UNDESIRED SIGNAL EXCEEDS VARIOUS VALUES AT A POINT WHERE INTERFERENCE IS MARGINAL BY PRESENT STANDARDS, I.E. WHERE THE VALUE EXCEEDED BY THE UNDESIRED ON 10% OF THE NIGHTS IS 1/20 THE VALUE EXCEEDED ON 50% OF THE NIGHTS BY THE DESIRED SIGNAL.

B THESE FUNCTIONS ARE SIMILAR BUT WITH THE ADDED RESTRICTION THAT THE DESIRED SIGNAL EXCEEDS 500 UV/M ON ONLY 50% OF THE NIGHTS AND ONLY THOSE NIGHTS ARE COUNTED WHEN THE RATIO EXCEEDS A SPECIFIED VALUE AND, SIMULTANEOUSLY, THE DESIRED IS GREATER THAN 500 UV/M.

FIGURE 6.3

FIGURE 6.3

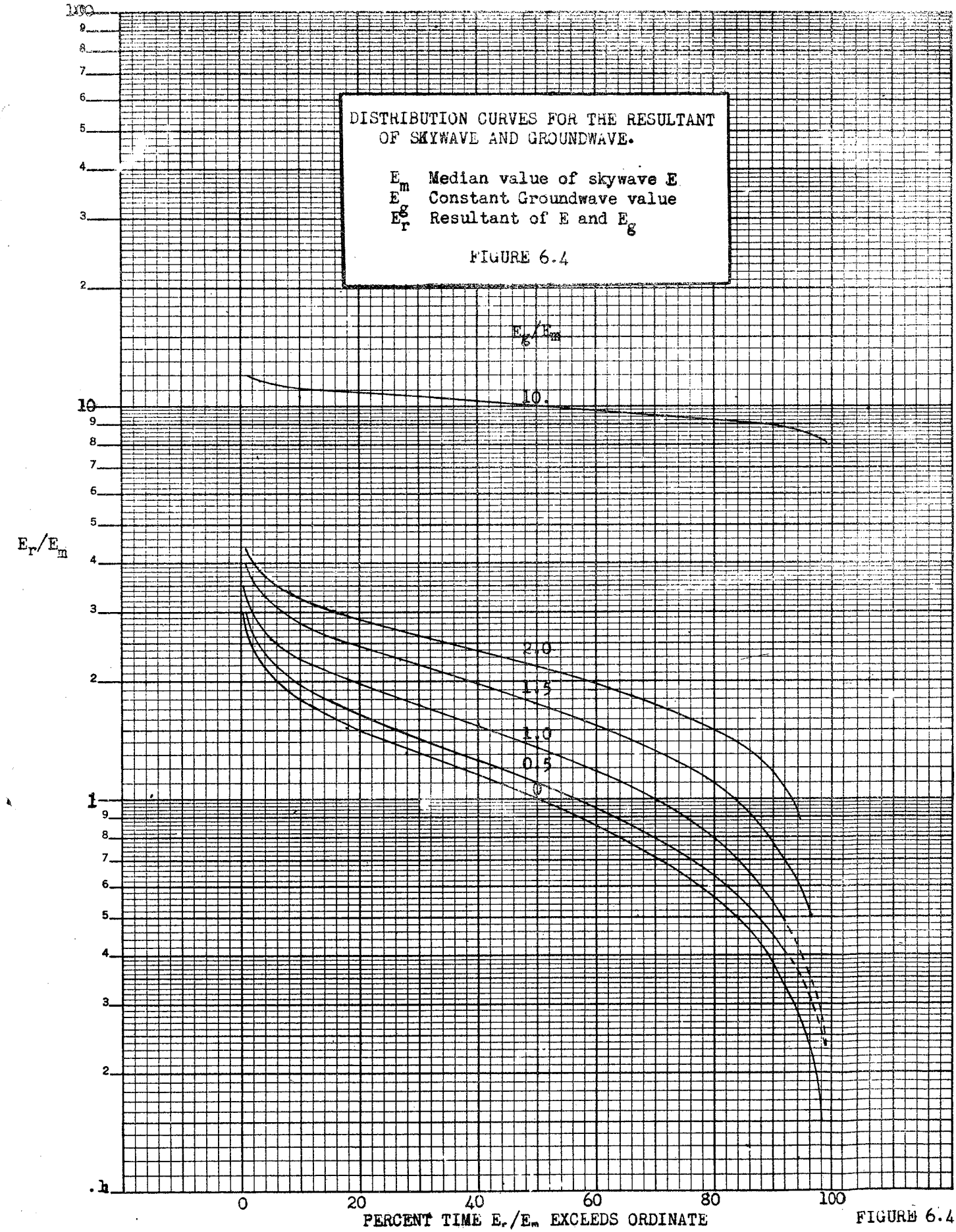
DISTRIBUTION CURVES FOR THE RESULTANT OF SKYWAVE AND GROUNDWAVE.
E_m Median value of skywave E
E_g Constant Groundwave value
E_r Resultant of E and E_g
FIGURE 6.4
E_g/E_m
10.
2.0
1.5
1.0
0.5
0
E_r/E_m
100
10
1
.1
0
20
40
60
80
100
PERCENT TIME E_r/E_m EXCEEDS ORDINATE

FIGURE 6.4